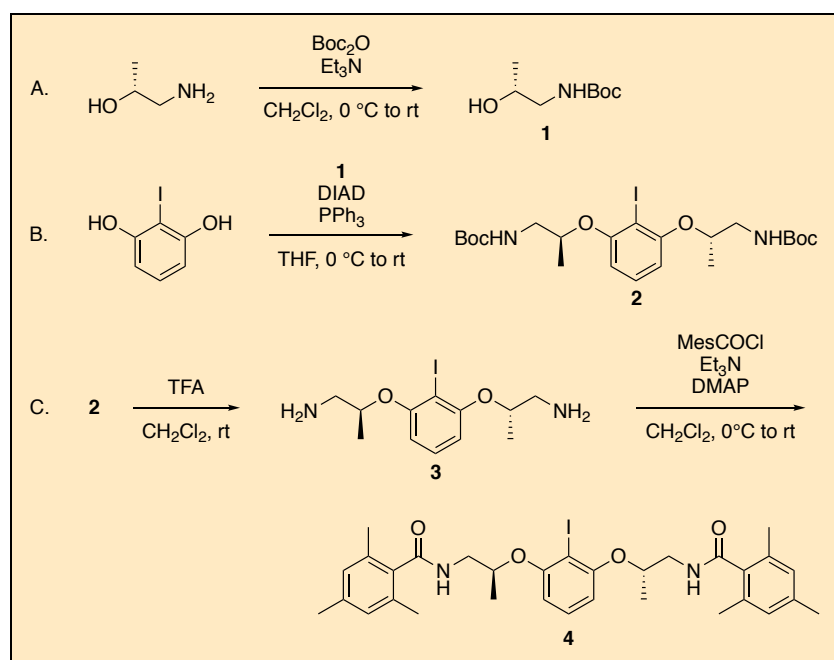


## Synthesis of Chiral Organoiodine Catalyst for Enantioselective Oxidative Dearomatization Reactions: *N,N'*-(2*S*,2'*S*)-(2-Iodo-1,3-phenylene)bis(oxy)bis(propane- 2,1-diyl)bis(2,4,6-trimethylbenzamide)

Muhammet Uyanik, Shinichi Ishizaki and Kazuaki Ishihara\*<sup>1</sup>

Graduate School of Engineering, Nagoya University, Furo-cho, Chikusa,  
Nagoya 464-8603, Japan

Checked by Cayetana Zarate and Kevin Campos



**Procedure (Note 1)**

A. *tert*-Butyl (*R*)-(2-hydroxypropyl)carbamate (**1**). A 250 mL, two-necked (main 24/40, side 24/40 joints), round-bottomed flask is equipped with a 25 x 8 mm, Teflon-coated magnetic stir bar, a 10-mL graduated, pressure-equalizing addition funnel fitted with a rubber septum at the top, and an inlet adapter with 3-way stopcock (Note 2) (Figure 1A). The set-up is evacuated under high vacuum (5.0 mmHg, few seconds) and filled with nitrogen (three cycles). Under a positive pressure of nitrogen, the flask is charged with (*R*)-1-amino-2-propanol (3.90 mL, 49.3 mmol, 1.0 equiv) (Note 3), triethylamine (7.24 mL, 52 mmol, 1.04 equiv) (Note 4), and CH<sub>2</sub>Cl<sub>2</sub> (38 mL) (Note 5) via syringe in less than 1 minute each through the inlet adapter. The flask is immersed in an ice-water bath (0 °C) and the mixture is stirred at 500 rpm for 10 min under a nitrogen atmosphere while the addition funnel is closed and charged with di-*tert*-butyl dicarbonate (Boc<sub>2</sub>O, 11.8 mL, 51.5 mmol, 1.03 equiv) (Note 6). Boc<sub>2</sub>O is added dropwise to the stirring mixture at 0 °C over 20 min via the addition funnel (Figure 1B). The inside wall of the addition funnel is washed with CH<sub>2</sub>Cl<sub>2</sub> (2 mL) via a syringe. The colorless reaction mixture is allowed to warm to 26 °C, and the resulting mixture is stirred at 400 rpm for 5 h at 26 °C (Note 7). The resulting colorless solution (Figure 1C) is concentrated by rotary evaporator (30 °C, 15 mmHg) resulting in a colorless oil. The crude material (Figure 1D) is further purified by flash column chromatography (Note 8) (Figures 1E–G) to give **1** (8.16 g, 46.6 mmol, 93%) as a colorless oil (Notes 9, 10, and 11) (Figure 1H).

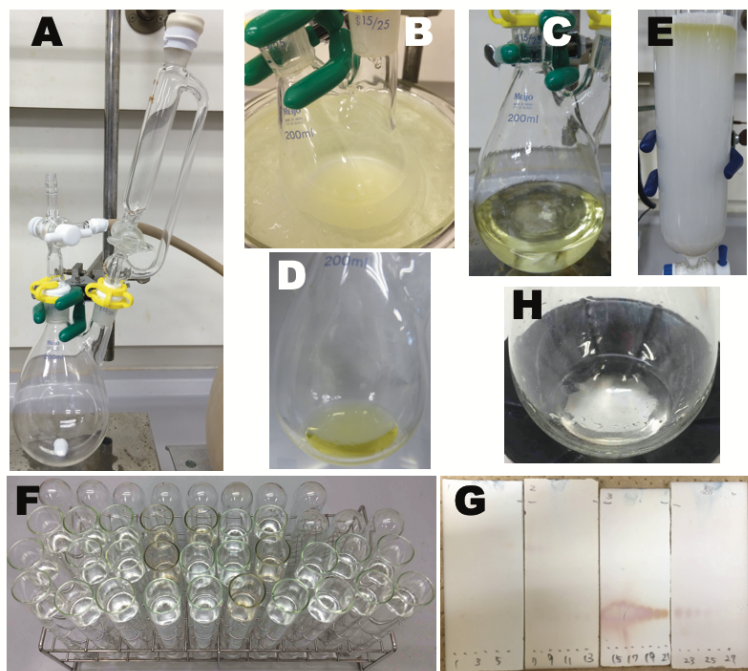


**Figure 1. Synthesis of compound 1; (A) Reaction setup; (B,C) Reaction progress; (D) Crude product; (E) Column chromatography (the checkers used a Combi-flash system); (F) Fractions; (G) TLC of fractions; (H) Pure product 1 (photos provided by submitters)**

B. *Di-tert-butyl ((2*S*,2'*S*)-((2-iodo-1,3-phenylene)bis(oxy))bis(propane-2,1-diyl))dicarbamate (2)*. A 250 mL, two-necked (main 24/40, side 24/40 joints), round-bottomed flask is charged with **1** (6.86 g, 40.0 mmol, 2.5 equiv), 2-iodoresorcinol (3.78 g, 16.0 mmol, 1.0 equiv) (Note 12), and triphenylphosphine (10.5 g, 40.0 mmol, 2.5 equiv) (Note 13), and the flask is equipped with a 25x8 mm, Teflon-coated magnetic stir bar, a 60-mL graduated, pressure-equalizing addition funnel fitted with a rubber septum at the top, and a rubber septum with an inlet connected to a nitrogen Schlenk line (Note 2) (Figure 2A). The whole system is evacuated under high vacuum (5.0 mmHg, few seconds) and filled with nitrogen (three cycles). Under a positive pressure of nitrogen, THF (48.0 mL) (Note 14) is added via a syringe in less than 1 minute through the rubber septum. The flask is immersed in an ice-water bath (0 °C) and the mixture is stirred at 500 rpm for 10 min under a nitrogen atmosphere while the addition funnel is closed and charged with

diisopropyl azodicarboxylate (DIAD, 1.9 M in toluene, 21.1 mL, 40.0 mmol, 2.5 equiv) (Note 15). DIAD is added dropwise to the stirring mixture over 40 min via the addition funnel at 0 °C (Figure 2B). The inside wall of the addition funnel is washed with THF (2 mL) via syringe. The reaction mixture is allowed to warm, and the mixture is stirred at 500 rpm for 13 h at 26 °C (Note 16). The resulting clear pale-yellow solution (Figure 2C) is concentrated by rotary evaporator (30 °C, 15 mmHg) for 15 min until about ca. 30 mL remains. To precipitate the byproducts (phosphine oxide and hydrazine derivatives), hexanes (30 mL) (Note 17) is added and the resulting mixture is stirred at 500 rpm for 5 min to make a slurry, which is then concentrated by rotary evaporator (30 °C, 15 mmHg) for additional 5 min. To further precipitate the byproducts, Et<sub>2</sub>O (10 mL) (Note 18) and hexanes (30 mL) (Note 17) are added and the resulting mixture is stirred at 500 rpm for 5 min to make a slurry. The resulting mixture is filtered through a plug of tightly packed celite (3 g) pre-wetted with Et<sub>2</sub>O (30 mL) (Note 18) on a sintered glass funnel (4 cm diameter, medium porosity) under vacuum suction (Figure 2D). The flask is rinsed with Et<sub>2</sub>O (50 mL) (Note 16) and this rinse is used to wash the precipitate. The wet-cake is further washed with Et<sub>2</sub>O (ca. 200 mL) (Note 18). The filtrate, collected in a 500-mL round-bottomed flask, is concentrated by rotary evaporator (30 °C, 40 mmHg). The crude residue (Figure 2E) is purified by column chromatography (Note 19) (Figure 2F–H) to give **2** as a colorless amorphous solid (8.12 g, 14.8 mmol, 93%) (Notes 20, 21, and 22) (Figure 2I), which is used in the next step.

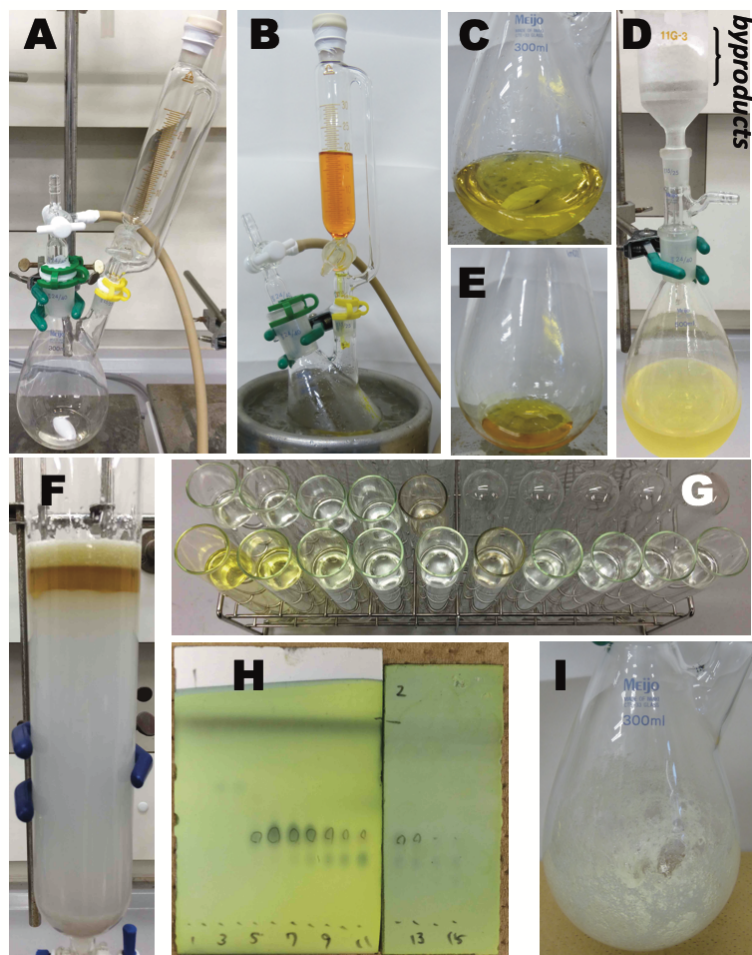


**Figure 2. Synthesis of compound 2; (A) Reaction setup; (B, C) Reaction progress; (D) Filtration; (E) Crude product; (F) Column chromatography; (G) Fractions; (H) TLC of fractions; (I) Pure product 2 (photos provided by submitters)**

C. *N,N'*-((2*S*,2'*S*)-((2-Iodo-1,3-phenylene)bis(oxy))bis(propane-2,1-diyl))bis-(2,4,6-trimethylbenzamide) (**4**). A 500 mL, two-necked (24/40), round-bottomed flask is charged with **2** (as obtained from step B) and the flask is equipped with a 25 x 8 mm, Teflon-coated magnetic stir bar, an inlet adapter with 3-way stopcock fitted with a nitrogen inlet (Note 2) (Figure 3A). The setup is evacuated under high vacuum (5.0 mmHg, few seconds) and filled with

nitrogen (three cycles). Dichloromethane (75 mL) (Note 5) (Figure 3B) and trifluoroacetic acid (11.0 mL, 143 mmol, 10.1 equiv) (Note 23) (Figure 3C) are added via syringe over ca. 1 min and 5 min, respectively, through the rubber septum at 23 °C. The resulting mixture is stirred at 500 rpm for 6 h at 26 °C (Note 24). The resulting pale brown suspension (Figure 3D) is cooled to 0 °C in an ice-bath and quenched with 2 M NaOH (80 mL, pH 13) (Note 25) (Figure 3E). The mixture is transferred to a 200 mL separatory funnel. The aqueous layer is separated and extracted with CH<sub>2</sub>Cl<sub>2</sub> (8 x 80 mL) (Notes 26 and 27) (Figure 3F). The combined organic layers are transferred to a 1 L separatory funnel and washed with saturated brine (150 mL) (Note 28), dried over anhydrous Na<sub>2</sub>SO<sub>4</sub> (60 g) (Note 29), and filtered through a sintered glass funnel (6.5 cm diameter, medium porosity) under vacuum suction. The filtrate is concentrated by rotary evaporation (30 °C, 15 mmHg) and dried under vacuum (23 °C, 5 mmHg, 13 h) to give **3** as an orange oil (4.99 g, including some impurities) (Figure 3G), which is used in the next step without further purification (Note 30).

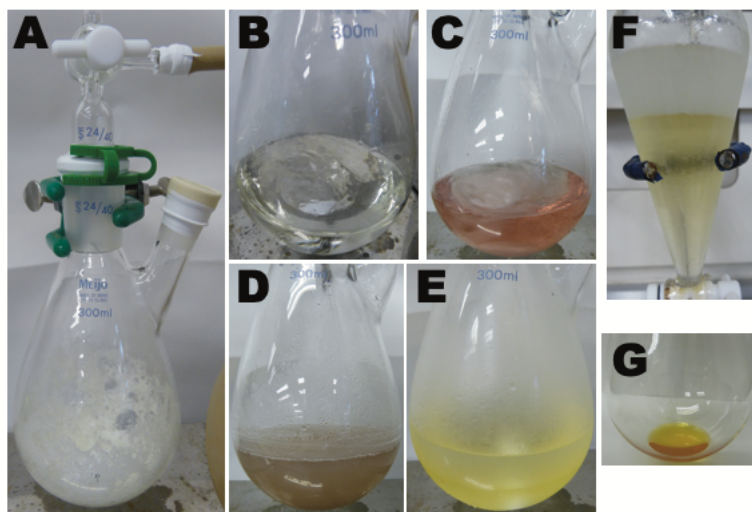


**Figure 3. Synthesis of compound 3; (A) Reaction setup; (B–D) Reaction progress with color changing; (E) Quenching; (F) Work-up; (G) Crude product 3 (photos provided by submitters)**

A 250 mL, two-necked (main 24/40, side 15/25 joints), round-bottomed flask equipped with a 3.5 cm, Teflon-coated magnetic stir bar is charged with

3 (as obtained from previous reaction) and 4-dimethyl aminopyridine (3.81 g, 31.2 mmol, 2.2 equiv) (Note 31) and the flask is equipped with a 20-mL graduated, pressure-equalizing addition funnel fitted with a rubber septum at the top, and an inlet adapter with 3-way stopcock connected to a nitrogen Schlenk line (Note 2) (Figure 4A). The set-up is evacuated under high vacuum (5.0 mmHg, few seconds) and filled with nitrogen (three cycles).  $\text{CH}_2\text{Cl}_2$  (100 mL) (Note 5) and triethyl amine (6.58 mL, 46.8 mmol, 3.0 equiv) (Note 4) are added via syringe in less than 1 minute each through the inlet adapter. The flask is immersed in an ice-water bath at 0 °C and stirred at 500 rpm for 10 min under a nitrogen atmosphere while the addition funnel is closed and charged with 2,4,6-trimethylbenzoyl chloride (MesCOCl, 54.6 mmol, 9.07 mL, 3.5 equiv) (Note 32). MesCOCl is added dropwise for ca. 7 min to the stirring mixture via the addition funnel at 0 °C (Figure 4B). The inside wall of the addition funnel is washed with  $\text{CH}_2\text{Cl}_2$  (2 mL) via syringe. The reaction mixture is allowed to warm to 26 °C, and the resulting mixture is stirred at 500 rpm for 13 h at 26 °C (Note 33). The resulting clear yellow solution (Figure 4C) is cooled to 0 °C and quenched with 1 M HCl (70 mL, pH = 1) (Note 34) (Figure 4D). The mixture is transferred to a 300 mL separatory funnel. The aqueous layer is separated and extracted with  $\text{CH}_2\text{Cl}_2$  (2 x 80 mL) (Note 26) (Figure 4E). The combined organic layers are transferred to a 500 mL separatory funnel, washed with saturated aqueous  $\text{NaHCO}_3$  (100 mL) (Note 35) (Figure 4F) and saturated brine (100 mL) (Note 28), and dried over anhydrous  $\text{Na}_2\text{SO}_4$  (40 g) (Note 29). The combined organic layers are filtered through a sand (Note 36), celite (Note 37), silica gel (Note 38) and 3-aminopropyl-functionalized silica gel (NH silica) (Note 39) pad (Note 40) on a sintered glass funnel (6.5 cm diameter, medium porosity) under vacuum suction, and the pad is washed with  $\text{CH}_2\text{Cl}_2$  (100 mL) (Note 26) followed by EtOAc (200 mL) (Note 41) (Figure 4G). The filtrate (Figure 4H) is concentrated by rotary evaporation (30 °C, 15 mmHg) and dried under vacuum (23 °C, 5.0 mmHg, 1 h). The crude yellow residue (Figure 4I) is recrystallized (Note 42) from toluene (Note 43) at -20 °C to provide 4 (3.90–4.59 g, 6.06–7.14 mmol) as a pale white solid. The filtrate from the crystallization was evaporated and the resulting solid recrystallized (Note 44) from toluene (Note 43) to provide a second batch of 4 (1.88–2.62 g, 2.93–4.08 mmol) as a pale white solid. The two crops of recrystallized product were combined to give 4 (6.47 g, 10.07 mmol, 66%) as a pale white solid (Figure 4J) (Notes 45, 46, and 47).

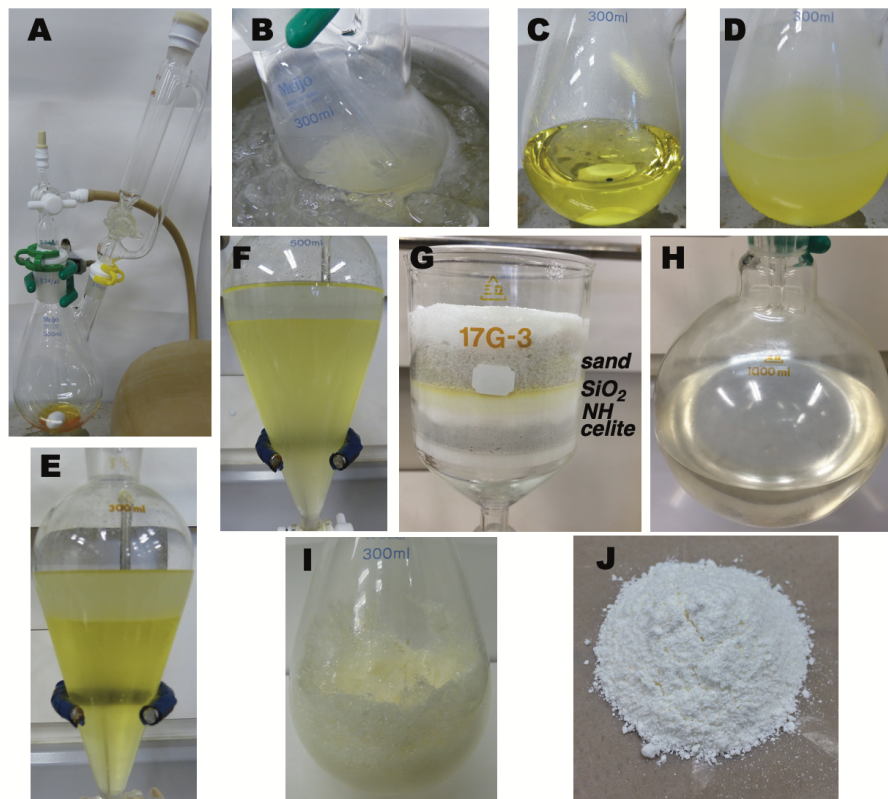


Figure 4. Synthesis of compound 4; (A) Reaction setup; (B, C) Reaction progress; (D) Quenching; (E–H) Work-up; (I) Crude; (J) Pure product 4 (photos provided by submitters)

## Notes

1. Prior to performing each reaction, a thorough hazard analysis and risk assessment should be carried out with regard to each chemical substance and experimental operation on the scale planned and in the context of the laboratory where the procedures will be carried out. Guidelines for carrying out risk assessments and for analyzing the hazards associated with chemicals can be found in references such as Chapter 4 of "Prudent Practices in the Laboratory" (The National Academies Press, Washington, D.C., 2011; the full text can be accessed free of charge at

<https://www.nap.edu/catalog/12654/prudent-practices-in-the-laboratory-handling-and-management-of-chemical>. See also "Identifying and Evaluating Hazards in Research Laboratories" (American Chemical Society, 2015) which is available via the associated website "Hazard Assessment in Research Laboratories" at <https://www.acs.org/content/acs/en/about/governance/committees/chemicalsafety/hazard-assessment.html>. In the case of this procedure, the risk assessment should include (but not necessarily be limited to) an evaluation of the potential hazards associated with (*R*)-1-amino-2-propanol, triethyl amine, dichloromethane, nitrogen, di-*tert*-butyl dicarbonate, silica gel, hexanes, ethyl acetate, chloroform, 2-iodoresorcinol, triphenylphosphine, tetrahydrofuran, diisopropyl azodicarboxylate, toluene, hexanes, ethyl acetate, diethyl ether, trifluoroacetic acid, sodium hydroxide, sodium chloride, sodium sulfate, 4-dimethyl aminopyridine, 2,4,6-trimethylbenzoyl chloride, hydrogen chloride and sodium hydrogen carbonate as well as the proper procedures for experimental operations.

2. The reaction was performed under a positive pressure of nitrogen gas by using a Schlenk line.
3. (*R*)-1-Amino-2-propanol (>97.0%) was purchased from Angene and used as received.
4. Triethylamine (98.0%) was purchased from Apollo Scientific and used as received.
5. Dichloromethane (anhydrous, 99.5%) was purchased from Acros Organics and used as received.
6. Di-*tert*-butyl dicarbonate (>95.0%) was purchased from Apollo Scientific and used as received.
7. The reaction progress was monitored by TLC analysis (TLC Silica gel 60 F254, pre-coated plates (0.25 mm) purchased from Merck) (visualized with ninhydrin stain solution in EtOH/AcOH) with EtOAc/hexanes (1:1) as eluent. Product  $R_f = 0.31$ , starting material  $R_f = 0.00$ .
8. The product **1** was purified by flash column chromatography in a Teledyne ISCO CombiFlash instrument using a RediSep<sup>®</sup> RF 120 g gold silica column, a gradient of EtOAc/hexanes from 15% to 50% and a flow rate of 85 mL/min. Hexanes and EtOAc were purchased from Acros Organics and used as received. The reaction crude oil was added to a RediSep<sup>®</sup> RF 12 g silica cartridge and the residue in the flask was transferred to the cartridge with hexanes (1 mL). The cartridge was then connected to the column. The product was eluted with 1.0 L of

hexanes/EtOAc (15% EtOAc) followed by 1.0 L of hexanes/EtOAc (50% EtOAc). The column chromatography was monitored by TLC analysis (TLC Silica gel 60 F254, pre-coated plates (0.25 mm) purchased from Merck) (visualized with ninhydrin stain solution in EtOH/AcOH) with EtOAc/hexanes (1:1) as eluent. Product  $R_f = 0.31$ . Fractions (25 x 150 mm, 50 mL) 27–39 were collected and concentrated by rotary evaporation (30 °C, 15 mmHg) and dried under high vacuum (23 °C, 5.0 mmHg, 40 h). Product **1** was used in step B.

9. *tert*-Butyl (*R*)-(2-hydroxypropyl)carbamate (**1**):  $^1\text{H}$  NMR ( $\text{CDCl}_3$ , 600 MHz):  $\delta$ : 1.17 (d,  $J = 6.3$  Hz, 3H), 1.44 (s, 9H), 2.30 (br s, 1H), 2.99 (dd,  $J = 14.0, 7.5$  Hz, 1H), 3.15–3.34 (m, 1H), 3.89 (ddq,  $J = 9.5, 6.4, 3.2$  Hz, 1H), 4.95 (br s, 1H);  $^{13}\text{C}$  NMR ( $\text{CDCl}_3$ , 151 MHz)  $\delta$ : 20.8, 28.5, 48.2, 67.8, 79.8, 156.9; IR (film): 3362, 2974, 1685, 1159, 761, 691  $\text{cm}^{-1}$ ;  $[\alpha]^{20}_{\text{D}} = -359$  ( $c$  1.11,  $\text{CHCl}_3$ ); Anal. Calcd. For  $\text{C}_8\text{H}_{17}\text{NO}_3$ : C, 54.84; H, 9.78; N, 7.99. Found: C, 53.47; H, 9.71; N, 7.73.
10. The purity of compound **1** (98%) was determined by quantitative  $^1\text{H}$  NMR analysis using compound **1** (29.33 mg, 0.167 mmol) and 1,2,4,5-tetramethylbenzene (20.66 mg, 0.154 mmol) as an internal standard.
11. A second reaction on the same scale provided 8.32 g (95%) of the product with identical purity.
12. 2-Iodoresorcinol (>97.0%) was purchased from Combi-Blocks. This compound was purified prior use to provide high yield. To this compound (5.13–5.27 g) was added  $\text{CHCl}_3$  (6 mL) at  $-10$  °C, and the solids were collected by suction filtration on a 60 mL sintered glass funnel (24/40 frit, fine porosity), washed with cold ( $-10$  °C)  $\text{CHCl}_3$  (6 mL) and dried under vacuum (23 °C, 5.0 mmHg, 5 h) to give a pure compound.
13. Triphenylphosphine (>97.0%) was purchased from Combi-Blocks and used as received.
14. THF (anhydrous, 99.5%) was purchased from Acros Organics and used as received.
15. Diisopropyl azodicarboxylate (DIAD) was purchased from eMolecules, Inc. and a 1.9 M solution in toluene was prepared dissolving DIAD (11.1 mL, 56.3 mmol) in 30 mL toluene. Toluene (anhydrous) was purchased from Acros Organics and used as received.
16. The reaction progress was monitored by TLC analysis (TLC Silica gel 60 F254, pre-coated plates (0.25 mm) purchased from Merck) (visualized with ninhydrin) with EtOAc/hexanes (1:2) as eluent. Product  $R_f = 0.49$ , starting material  $R_f = 0.29$ .

17. Hexanes ( $\geq 95.0\%$ ) was purchased from Acros Organics and used as received.
18. Diethyl ether ( $\geq 99.5\%$ ) was purchased from Sigma-Aldrich and used as received.
19. Product 2 was purified by flash column chromatography in a Teledyne ISCO CombiFlash instrument using a RediSep<sup>®</sup> RF 120 g gold silica column, a gradient of EtOAc/hexanes from 10% to 20%, and a flow rate of 85 mL/min. The reaction crude was charged to a RediSep<sup>®</sup> Rf 12 g silica cartridge that later was connected to the column. The product was eluted with 1.5 L of hexanes/EtOAc (10% EtOAc) followed by 1.5 L of hexanes/EtOAc (20% EtOAc). The column chromatography was monitored by TLC analysis (TLC Silica gel 60 F254, pre-coated plates (0.25 mm) purchased from Merck) (visualized with 254 nm UV lamp and phosphomolybdic acid stain solution) with EtOAc/hexanes (1:2) as eluent. Product  $R_f = 0.49$ . The fractions (25x150 mm, 50 mL) 32-51 were collected and concentrated by rotary evaporation (30 °C, 15 mmHg), and dried under high vacuum (23 °C, 5.0 mmHg, 40 h) to give compound 2.
20. Di-*tert*-butyl ((2*S*,2'*S*)-((2-iodo-1,3-phenylene)bis(oxy))bis(propane-2,1-diyl))dicarbamate (**2**): <sup>1</sup>H NMR (CDCl<sub>3</sub>, 600 MHz)  $\delta$ : 1.33 (d,  $J = 6.2$  Hz, 6H), 1.43 (s, 18H), 3.31 (dt,  $J = 13.5, 6.2$  Hz, 2H), 3.59 – 3.46 (m, 2H), 4.58 – 4.43 (m, 2H), 5.09 (br s, 2H), 6.50 (d,  $J = 8.3$  Hz, 2H), 7.20 (t,  $J = 8.2$  Hz, 1H); <sup>13</sup>C NMR (CDCl<sub>3</sub>, 151 MHz)  $\delta$ : 17.3, 28.5, 45.8, 75.5, 79.6, 82.4, 107.3, 129.9, 156.3, 158.1; LC/MS analysis (Agilent 1200 instrument with an Inductively Coupled Plasma (IPC)):  $m/z$  (relative intensity): 573 (97.35%);  $[\alpha]_D^{20} = +87.0$  ( $c$  0.02, CHCl<sub>3</sub>); Anal. Calcd. For C<sub>22</sub>H<sub>35</sub>IN<sub>2</sub>O<sub>6</sub>: C, 48.01; H, 6.41; N, 5.09. Found: C, 47.59; H, 6.06; N, 4.72.
21. The purity of compound 2 (96%) was determined by quantitative <sup>1</sup>H NMR analysis using compound 2 (6.5 mg, 11.81  $\mu$ mol) and 1,2,4,5-tetramethylbenzene (9.6 mg, 71.56  $\mu$ mol) as an internal standard. SFC CHIRALCEL<sup>®</sup> OD-3 (3.0  $\mu$ m, 150 x 4.6 mm) column, MP A: CO<sub>2</sub>, MP B: 25 mM isobutylamine (IBA) in ethanol, column temperature: 40 °C, wavelength: PDA, pressure: 2600 psi, flow rate: 2.5 mL/min, gradient as below,  $t_R = 2.10$  min (R),  $t_S = 2.51$  min (S), small impurity detected (<4% by UV analysis).
22. A second reaction on the same scale provided 8.44 g (15.3 mmol, 95%) of the product.
23. Trifluoroacetic acid (>99.0%) was purchased from Oakwood Chemical and used as received. Equivalencies were based upon the amount of starting material, corrected for purity (Note 21).

24. The reaction progress was monitored by TLC analysis (TLC Silica gel 60 F254, pre-coated plates (0.25 mm) purchased from Merck) (visualized with 254 nm UV lamp and molybdato-phosphoric acid) with EtOAc/hexanes (1:2) as eluent. Product  $R_f = 0.02$ , starting material  $R_f = 0.49$ .
25. NaOH ( $\geq 97.0\%$ ) was purchased from Fisher Chemical and used as received. 2M NaOH solution was prepared using deionized water. Control of pH was crucial for extracting compound **3** from aqueous phase during work-up.
26. Dichloromethane (99.0%) for work-up was purchased from Acros Organics and used as received.
27. The aqueous layer was extracted eight times to remove completely the diamine product from the aqueous layer.
28. Sodium chloride ( $>99.0\%$ ) was purchased from Fisher Chemical and used as received. Saturated brined solution was prepared using deionized water.
29. Sodium sulfate, anhydrous ( $>99\%$ ) was purchased from Fisher Chemical and used as received.
30. Compound **3** containing small impurities was obtained as a pale orange oil:  $^1\text{H NMR}$  ( $\text{CDCl}_3$ , 600 MHz)  $\delta$ : 1.18 (d,  $J = 6.2$  Hz, 6H), 2.73 – 2.85 (m, 4H), 3.58 (s, 3H (integration value of  $\text{NH}_2$  is low), 4.25 (h,  $J = 6.0$  Hz, 2H), 6.36 (d,  $J = 8.3$  Hz, 2H), 7.06 (t,  $J = 8.2$  Hz, 1H);  $^{13}\text{C NMR}$  ( $\text{CDCl}_3$ , 151 MHz)  $\delta$ : 17.3, 47.7, 77.8, 82.3, 106.8, 129.6, 158.4 (a resonance arising from an impurity appears at approximately 28 ppm);  $[\alpha]_{\text{D}}^{30.3} = 84.0$  ( $c$  0.50,  $\text{CHCl}_3$ ); Anal. Calcd. For  $\text{C}_{12}\text{H}_{19}\text{N}_2\text{O}_2$ : C, 41.16; H, 5.47; N, 8.00. Found: C, 41.02; H, 5.84; N, 7.25.
31. 4-Dimethylaminopyridine ( $>99.0\%$ ) was purchased from Oakwood Chemical and used as received.
32. 2,4,6-Trimethyl benzoyl chloride ( $>80\%$ ) was purchased from Angene and used as received.
33. The reaction progress was monitored by TLC analysis (TLC Silica gel 60 F254, pre-coated plates (0.25 mm) purchased from Merck) (visualized with 254 nm UV lamp) with MeOH/ $\text{CHCl}_3$  (1:30) as eluent. Product  $R_f = 0.72$ , starting material  $R_f = 0.39$ .
34. Concentrated HCl (35.0–37.0%) was purchased from Sigma-Aldrich and used as received. 1 M HCl solution was prepared using deionized water.
35.  $\text{NaHCO}_3$  (99.5–100.3%) was purchased from Fisher Chemical and used as received. Saturated aqueous  $\text{NaHCO}_3$  solution was prepared using deionized water.

36. Sand was purchased from Fisher Chemical and used as received.
37. Celite was purchased from Fisher Chemical and used as received.
38. Silica gel was purchased from Fisher Chemical and used as received.
39. 3-Aminopropyl-functionalized silica gel (NH silica) was purchased from Sigma-Aldrich and used as received.
40. From bottom to top, 10 g of celite, 10 g of 3-aminopropyl-functionalized silica gel (NH silica), 10 g of silica gel, and 60 g of sand were added to a sintered glass funnel and wetted with  $\text{CH}_2\text{Cl}_2$  (50 mL) (Figure 4G).
41. EtOAc (99%) was purchased from Acros Organics and used as received.
42. To a 250 mL round-bottomed flask containing the crude residue and a 2.5 cm, Teflon-coated magnetic stir bar was added toluene (80 mL), and the resulting mixture was heated to 110 °C with 500 rpm stirring in a silicone oil bath (Figure 5A). After 20 min, toluene (2 mL x 5 times) was added to the stirring cloudy solution at 110 °C every 5 minutes until the solids were dissolved completely (total toluene = 110 mL) (Figure 5B). The resulting clear yellow solution was removed from the oil bath,

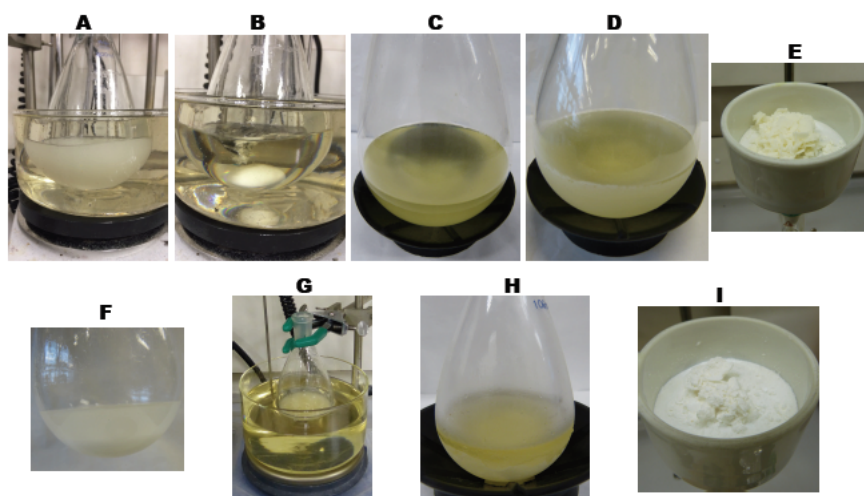


**Figure 5. Recrystallization of compound 4; 1<sup>st</sup> Round: (A) Stirring suspension with 100 mL toluene at 110 °C; (B) Clear solution (total amount of toluene added: 110 mL); (C) Before cooling; (D) After cooling at -20 °C; (E) Collected solids from 1<sup>st</sup> round; (F) Filtrate; 2<sup>nd</sup> Round: (G) Stirring suspension with 30 mL toluene at 110 °C; (H) After cooling at -20 °C; (I) Collected solids from 2<sup>nd</sup> round (photos provided by submitters)**

- stirring bar was removed, and the mixture was cooled to 23 °C for 30 min (Figure 5C). Crystal seeds of compound **4** were then added to the solution and the solution was cooled to -20 °C in a freezer for 16 h (Figure 5D). The resulting white solid was collected by suction filtration on a Büchner funnel (7 cm diameter) and washed with cold (-20 °C) toluene (40 mL) (Figure 5E). The resulting pale white solid was then transferred to a 200 mL round-bottomed flask and dried under vacuum for 16 h (110 °C, 5.0 mmHg) to give **4** (3.90 g, 6.06 mmol) as a pale white solid.
43. Toluene (99%) was purchased from Fisher Chemical and used as received.
44. The filtrate (Figure 5F) was concentrated by rotary evaporation (40 °C, 15 mmHg) and dried under vacuum (23 °C, 5.0 mmHg, 0.5 h). To a 100 mL round-bottomed flask containing the residue and a 2.5 cm, Teflon-coated magnetic stir bar was added toluene (30 mL), and the resulting mixture was heated to 110 °C with 500 rpm stirring (Figure 5G). After 20 min, additional toluene (2 mL x 5 times) was added to the stirring cloudy solution at 110 °C every 5 minutes until the solids were dissolved completely (total toluene = 40 mL). The stirring bar was removed, and the clear yellow solution was cooled to 23 °C for 30 min. Crystal seeds of compound **4** were added and the solution was cooled to -20 °C in a freezer for 16 h (Figure 5H). The resulting white solid was collected by suction filtration on a Büchner funnel (7 cm diameter) and washed with cold (-20 °C) toluene (40 mL) (Figure 5I). The solids were then transferred to a 100 mL round-bottomed flask and dried under vacuum for 16 h (110 °C, 5.0 mmHg) to provide a second batch of **4** (1.88 g, 2.93 mmol) as a pale white solid.
45. *N,N'*-((2*S*,2'*S*)-((2-Iodo-1,3-phenylene)bis(oxy))bis(propane-2,1-diyl))bis-(2,4,6-trimethylbenzamide) (**4**) has the following properties: mp 196–201 °C (decomposed); <sup>1</sup>H NMR (CDCl<sub>3</sub>, 600 MHz) δ: 1.40 (d, *J* = 6.2 Hz, 6H), 2.21 (s, 12H), 2.25 (s, 6H), 3.62 – 3.51 (m, 2H), 3.92 (ddd, *J* = 13.9, 6.7, 3.2 Hz, 2H), 4.74 – 4.63 (m, 2H), 6.21 (t, *J* = 5.5 Hz, 2H), 6.53 (d, *J* = 8.3 Hz, 2H), 6.80 (s, 4H), 7.22 (t, *J* = 8.3 Hz, 1H); <sup>13</sup>C NMR (CDCl<sub>3</sub>, 151 MHz) δ: 17.6, 19.3, 21.2, 44.6, 75.2, 82.4, 107.3, 128.4, 130.2, 134.2, 134.8, 138.6, 157.8, 171.0; IR (film): 3228, 2971, 2916, 2867, 1458, 1242, 1152, 879, 748 cm<sup>-1</sup>; LC/MS analysis (Agilent 1200 instrument with an Inductively Coupled Plasma (IPC)): *m/z* (relative intensity): 643 (97.10%); [α]<sub>D</sub><sup>20</sup> = +216.6 (c 0.038, CHCl<sub>3</sub>) for ~99% ee; Anal. Calcd. For C<sub>32</sub>H<sub>39</sub>IN<sub>2</sub>O<sub>4</sub>: C, 59.81; H, 6.12; N, 4.36. Found: C, 59.09; H, 6.02; N, 4.41.
46. The purity of compound **4** (99%) was determined by quantitative <sup>1</sup>H NMR analysis using compound **4** (15.4 mg, 0.024 mmol) and 1,2,4,5-

tetramethylbenzene (13.0 mg, 0.097 mmol) as an internal standard. SFC CHIRALCEL® OD-3 (3.0  $\mu\text{m}$ , 150 x 4.6 mm) column, MP A:  $\text{CO}_2$ , MP B: 25 mM isobutylamine (IBA) in ethanol, column temperature: 40  $^\circ\text{C}$ , wavelength: PDA, pressure: 2600 psi, flow rate: 2.5 mL/min, gradient as follows,  $t_{\text{R}} = 6.74$  min (R),  $t_{\text{RS}} = 7.12$  min (S), meso compound was detected in racemic sample.

47. A second run of Step C on the same scale provided 6.52 g (10.15 mmol, 68%) of the product.

## Working with Hazardous Chemicals

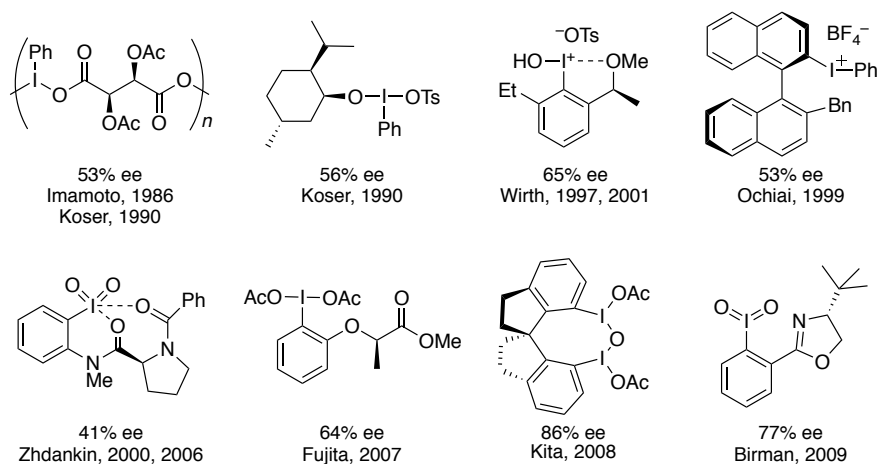
The procedures in *Organic Syntheses* are intended for use only by persons with proper training in experimental organic chemistry. All hazardous materials should be handled using the standard procedures for work with chemicals described in references such as "Prudent Practices in the Laboratory" (The National Academies Press, Washington, D.C., 2011; the full text can be accessed free of charge at [http://www.nap.edu/catalog.php?record\\_id=12654](http://www.nap.edu/catalog.php?record_id=12654)). All chemical waste should be disposed of in accordance with local regulations. For general guidelines for the management of chemical waste, see Chapter 8 of Prudent Practices.

In some articles in *Organic Syntheses*, chemical-specific hazards are highlighted in red "Caution Notes" within a procedure. It is important to recognize that the absence of a caution note does not imply that no significant hazards are associated with the chemicals involved in that procedure. Prior to performing a reaction, a thorough risk assessment should be carried out that includes a review of the potential hazards associated with each chemical and experimental operation on the scale that is planned for the procedure. Guidelines for carrying out a risk assessment and for analyzing the hazards associated with chemicals can be found in Chapter 4 of Prudent Practices.

The procedures described in *Organic Syntheses* are provided as published and are conducted at one's own risk. *Organic Syntheses, Inc.*, its Editors, and its Board of Directors do not warrant or guarantee the safety of individuals using these procedures and hereby disclaim any liability for any injuries or damages claimed to have resulted from or related in any way to the procedures herein.

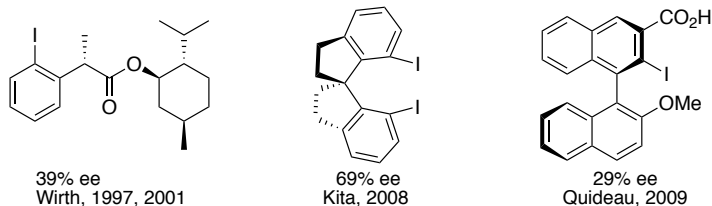
## Discussion

Despite its long history,<sup>2</sup> the development of enantioselective hypervalent organoiodine catalysis is one of the most challenging areas in asymmetric synthesis.<sup>3</sup> Representative examples of chiral hypervalent iodine reagents that were used for various asymmetric oxidations before our first report are shown in Scheme 1 (the best enantioselectivities observed with these reagents are also shown).<sup>4</sup> However, the enantioselectivities of these reactions were moderate (<80%), except for Kita's reagent reported in 2008



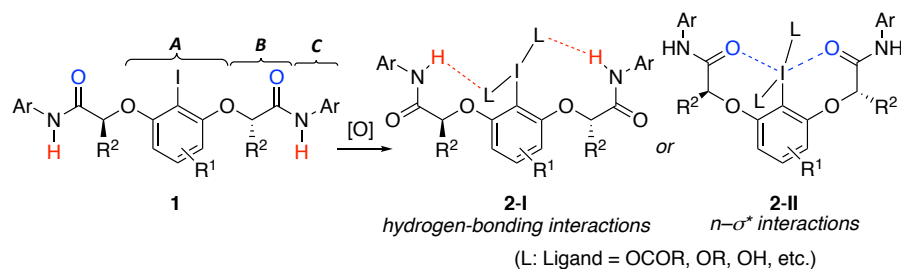
**Scheme 1. Representative chiral organoiodine (III or V) reagents reported before our first work<sup>4</sup>**

with 86% ee,<sup>5a</sup> which was the highest asymmetric induction using chiral hypervalent iodines reported at that time. Additionally, there have been only a few examples of *in situ*-generated chiral hypervalent organoiodine (III or V) catalysts with *m*-CPBA as a terminal oxidant (Scheme 2).<sup>5a,6a,6b</sup> In 2008, Kita's group designed a chiral hypervalent organoiodine catalyst with a conformationally rigid 1,1'-spirobiindane backbone, and applied this reagent to the enantioselective oxidative spirolactonization of 1-naphthol derivatives to the corresponding spirolactones with moderate enantioselectivity (up to 69% ee).<sup>5a</sup>



**Scheme 2. Chiral organoiodine catalysts used with *m*-CPBA as an oxidant reported before our first work<sup>5a,6a,6b</sup>**

In sharp contrast to Kita's conformationally rigid design, we reported the rational design of conformationally flexible hypervalent organoiodines as chiral catalysts based on secondary nonbonding interactions (i.e. intramolecular hydrogen-bonding interactions).<sup>7,8</sup> In 2010, we reported the design of conformationally flexible  $C_2$ -symmetric chiral iodoarenes **1** consisting of three units, including an iodoaryl moiety (**A**), chiral linkers (**B**), and subfunctional groups (**C**) (Scheme 3).<sup>7</sup> These units can be easily combined to give a wide variety of chiral iodoarenes **1**. Notably, the hypervalent iodines (III) **2** generated in situ from iodoarenes **1** were expected to exhibit intramolecular hydrogen-bonding interactions between the acidic hydrogen of **C** (NHAr) and the ligand (L, such as an acetoxy group, alkoxy

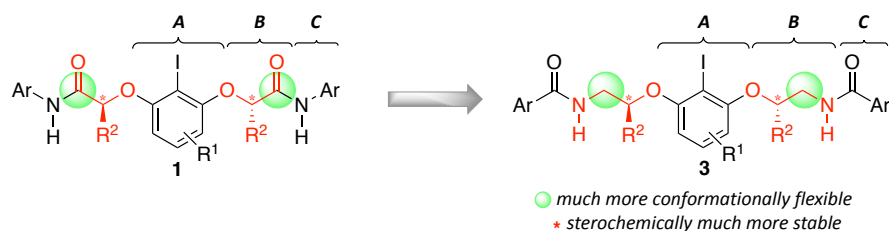


**Scheme 3. Design of our 1<sup>st</sup> generation conformationally flexible chiral organoiodine, **1****

group, hydroxy group, etc.) of iodine (III) (**2-I**). Alternatively, intramolecular  $n-\sigma^*$  interactions between the electron-deficient iodine (III) center ( $\sigma^*_{C-I}$  orbital) of **A** and the Lewis-basic group of **C** (lone pair  $n$ ), such as carbonyl groups, might also be generated (**2-II**). We envisioned that a suitable chiral environment might be constructed around the iodine (III) center of **2** via such non-covalent bonding intramolecular interactions. Our lactate-based<sup>4h</sup> 1<sup>st</sup>

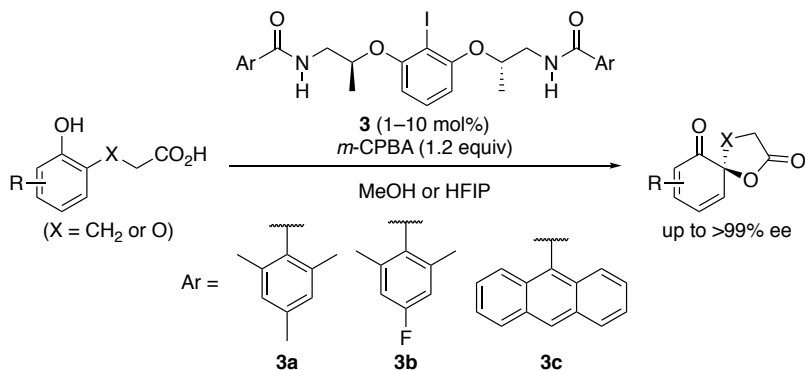
generation catalyst **1a** ( $R^1$ ,  $R^2$ , Ar = H, Me, Mes) could be successfully applied to the enantioselective oxidative dearomatization of 1-naphthol derivatives (Kita spirolactonization) to the corresponding spirolactones (up to 92% ee).

However, lactate-based catalysts **1** were found to be insufficient for the oxidation of phenols, which were less reactive than 1-naphthols, in terms of both reactivity and enantioselectivity. To overcome these limitations, we designed new chiral organoiodines **3**, 2<sup>nd</sup> generation catalysts, derived from 2-aminoalcohol instead of lactate as a chiral source (Scheme 4).<sup>8a</sup> As both **1** and **2** consist of 2-iodoresorcinol (**A**) and secondary amide (**C**) units, the corresponding acidic hydrogen atoms are at the same distance from the iodine center. On the other hand, because  $sp^2$ -hybridized carbonyl groups are moved to the outer sides, the 2<sup>nd</sup> generation catalysts **3** would be much more conformationally flexible. Moreover, **3** would be much more stereochemically stable than **1** as the stereocenters are far from the carbonyl groups.

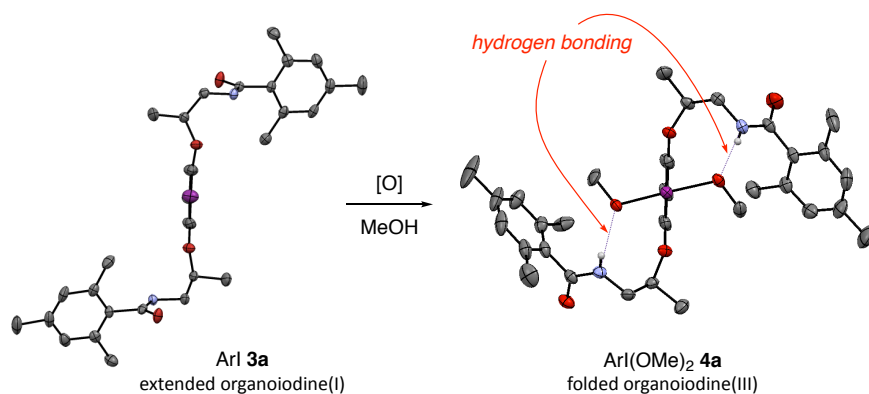


**Scheme 4. Design of 2<sup>nd</sup> generation organoiodines **3** using 2-aminoalcohol as a chiral source instead of lactate**

The enantioselective oxidation of not only 1-naphthols<sup>8b</sup> but also 2-naphthols<sup>8b</sup> and phenols<sup>8a</sup> as well as hydroquinone derivatives<sup>8c</sup> could be achieved by using organoiodine catalysts **3** ( $R^1$ ,  $R^2$  = H, Me) to give the corresponding cyclohexadienone spirolactones with excellent enantioselectivities up to 99% ee (Scheme 5). As an application of our enantioselective organoiodine catalysis, the asymmetric synthesis of (–)-maldoxin was achieved through the oxidative dearomatization of pestheic acid with excellent enantioselectivity.<sup>8d</sup> X-ray diffraction and NOE (Nuclear Overhauser Effect) NMR analyses of in situ-generated organoiodines (III) **4a** showed that a suitable chiral environment around the iodine (III) center was constructed via intramolecular hydrogen-bonding interactions (Scheme 6).<sup>8a</sup>



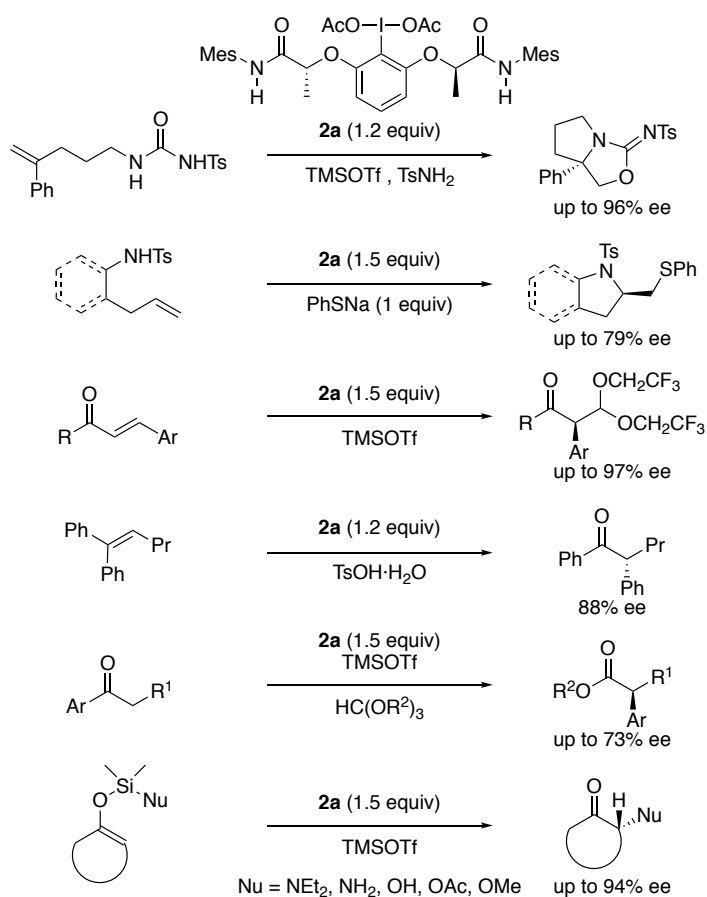
**Scheme 5. Enantioselective oxidative dearomatization of a variety of arenols using 2<sup>nd</sup> generation catalysts 3<sup>8</sup>**



**Scheme 6. X-ray structures of iodine (I) 3a and iodine (III) 4a<sup>8</sup>**

Our conformationally flexible 1<sup>st</sup> and 2<sup>nd</sup> generation organoiodines 1–3 could be successfully applied to a variety of enantioselective oxidative transformations as a reagent or catalyst.<sup>9–11</sup> Wirth's group reported a series of enantioselective oxidations using our secondary bisamide reagent **2a**<sup>7</sup> including the oxyamination of homoallylic urea derivatives to isoureas,<sup>9a</sup> intramolecular thioamination of alkenes to pyrrolines or indolines,<sup>9b</sup> oxidative rearrangements of chalcones<sup>9c</sup> or 1,1-disubstituted alkenes<sup>9d</sup> to  $\alpha$ -aryl ketones, oxidative rearrangement of arylketones in the presence of orthoesters to  $\alpha$ -arylesters,<sup>9e</sup> and intramolecular enantioselective

$\alpha$ -functionalization of carbonyl compounds through tethers between the nucleophile and silyl enol ethers<sup>9f</sup> (Scheme 7).

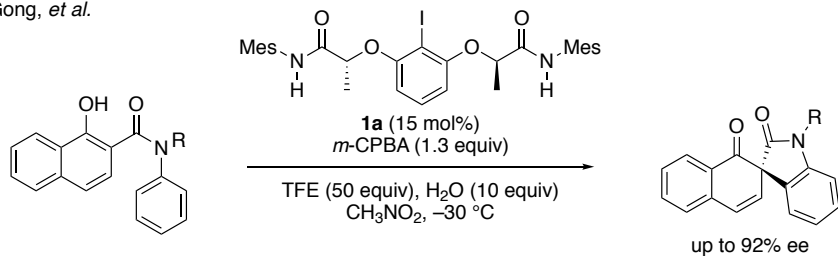


**Scheme 7. Enantioselective oxidative transformations using lactate-based chiral organoiodine (III) reagent **2a** reported by Wirth's group<sup>9</sup>**

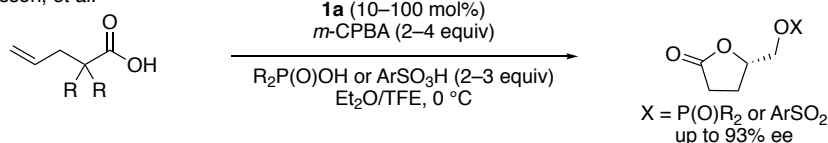
Enantioselective oxidations using catalytic amounts of iodoarenes **1** with an oxidant were also achieved (Scheme 8).<sup>10</sup> Gong's group reported the **1a**-catalyzed dearomatizative cyclization of 1-hydroxy-*N*-aryl-2-naphthamide derivatives to generate all-carbon spiro-stereocenter using *m*-CPBA as a stoichiometric oxidant.<sup>10a</sup> Masson's group reported the **1a**-catalyzed enantioselective sulfonyl- or phosphoryl-oxylactonization of 4-pentenoic

acids with *m*-CPBA to give the corresponding sulfonyloxy- or phosphoryloxy- $\gamma$ -butyrolactones.<sup>10b</sup> On the other hand, Muñiz and colleagues reported the intermolecular vicinal diacetoxylation of terminal styrenes using structurally congested secondary bisamide **1b** as a catalyst in the presence of peracetic acid as an oxidant.<sup>10c</sup> The same research group also reported the **1b**-catalyzed intermolecular dearomatization of phenols at the *para*-position using *m*-CPBA as an oxidant to give the corresponding *para*-quinols with moderate stereoselectivity.<sup>10d</sup>

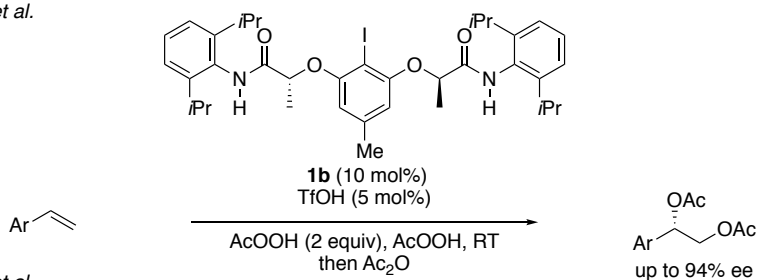
Gong, *et al.*



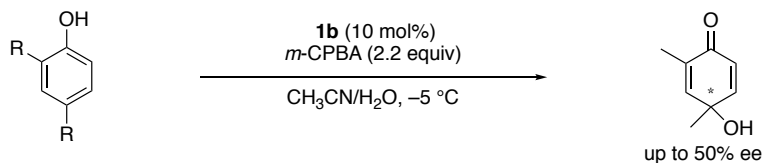
Masson, *et al.*



Muñiz *et al.*



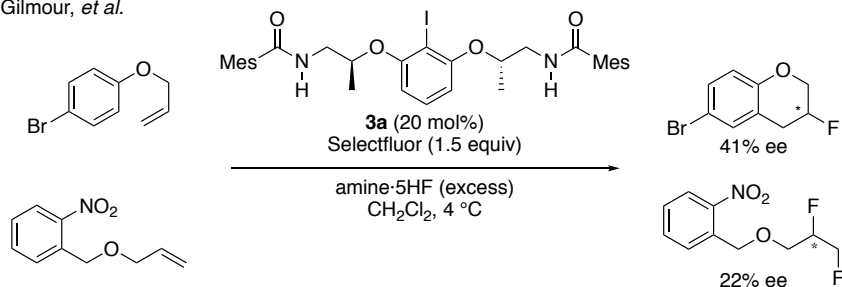
Muñiz *et al.*



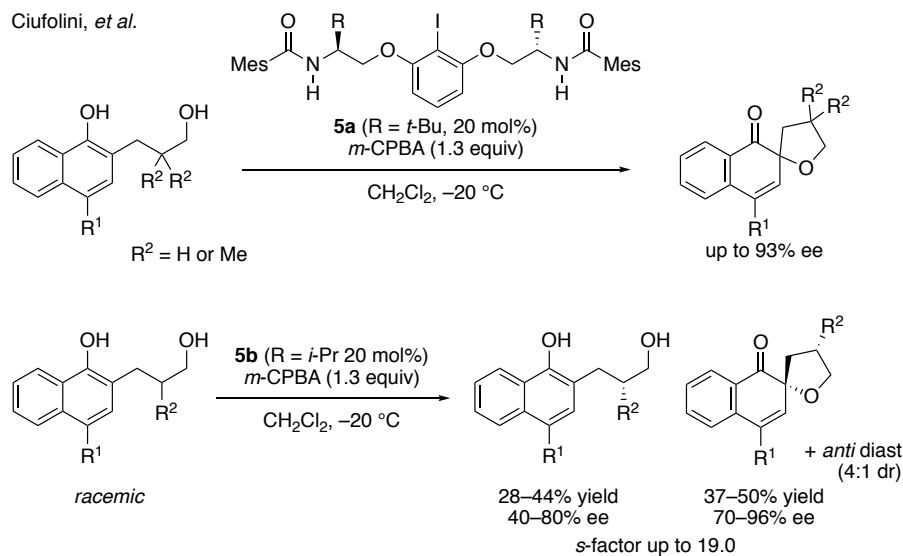
**Scheme 8. Enantioselective oxidative transformations using lactate-based chiral organoiodine(I) catalysts 1<sup>10</sup>**

On the other hand, 2<sup>nd</sup> generation catalysts **3** and their analogues **5** have also been applied to enantioselective oxidations (Scheme 9).<sup>11</sup> Gilmour and colleagues reported the enantioselective vicinal difluorination or fluorocyclization of terminal alkenes using *in situ*-generated aryliodonium difluoride species from a catalytic amount of **3a** with selectfluor as an oxidant in the presence of an excess amount of HF, albeit with only moderate enantioselectivity.<sup>11a</sup> Ciufolini and colleagues reported the enantioselective spiroetherification of 1-naphthol derivatives with *m*-CPBA as an oxidant to give the corresponding spiroethers with good to high enantioselectivities.<sup>11b</sup>

Gilmour, *et al.*



Ciufolini, *et al.*



**Scheme 9. Enantioselective oxidative transformations using amino alcohol-derived chiral organoiodine(I) catalysts **3** or **5**<sup>11</sup>**

Interestingly, catalyst **5a**, a structural analogue of our catalyst **3a**, was found to be superior to **3a** with respect to both stereoselectivity and reactivity for this particular reaction, especially under low catalyst-loading conditions.<sup>11b</sup> The same research group also reported the oxidative kinetic resolution of 1-naphtholic alcohols using catalyst **5b** with an *S*-factor of up to 19.0.<sup>11c</sup> These examples highlight the substantial scope of conformationally flexible designer organoiodine (III) catalysis.

## References

1. Graduate School of Engineering, Nagoya University, Furo-cho, Chikusa, Nagoya 464-8603, Japan. E-mail: ishihara@cc.nagoya-u.ac.jp. ORCID: 0000-0003-4191-3845. We thank JSPS.KAKENHI (15H05755 to K.I., 15H05484 to M.U., 18H01973 to M.U.), and the Program for Leading Graduate Schools: IGER Program in Green Natural Sciences (MEXT).
2. (a) Zhdankin, V. V. *Hypervalent Iodine Chemistry: Preparation, Structure and Synthetic Applications of Polyvalent Iodine Compounds*, Wiley, New York, 2014. (b) Kaiho, T., Ed.; *Iodine Chemistry and Application*, Wiley, Hoboken, New Jersey, 2015. (c) Wirth, T., Ed.; *Hypervalent Iodine Chemistry*; In *Top. Curr. Chem.* 373, Springer, Berlin, 2016. (d) Yoshimura, A.; Zhdankin, V. V. *Chem. Rev.* **2016**, *116*, 3328–3435.
3. (a) Lupton, D. W.; Ngatimin, M. *Aust. J. Chem.* **2010**, *63*, 653–658. (b) Liang, H.; Ciufolini, M. A. *Angew. Chem. Int. Ed.* **2011**, *50*, 11849–11851. (c) Uyanik, M.; Ishihara, K. *J. Synth. Org. Chem., Jpn.* **2012**, *70*, 1116–1122. (d) Parra, A.; Reboredo, S. *Chem. Eur. J.* **2013**, *19*, 17244–17260. (e) Harned, A. M. *Tetrahedron. Lett.* **2014**, *55*, 4681–4689. (f) Berthiol, F. *Synthesis* **2015**, 587–603. (g) Basdevant, B.; Guilbault, A.-A.; Beaulieu, S.; Lauriers, A. J.-D.; Legault, C. Y. *Pure Appl. Chem.* **2017**, *89*, 781–789.
4. (a) Imamoto, T.; Koto, H. *Chem. Lett.* **1986**, *15*, 967–968. (b) Ray, D. G.; Koser, G. F. *J. Org. Chem.* **1992**, *57*, 1607–1610. (c) Ray, D. G.; Koser, G. F. *J. Am. Chem. Soc.* **1990**, *112*, 5672–5673. (d) Wirth, T.; Hirt, U. H. *Tetrahedron: Asymmetry* **1997**, *8*, 23. (e) Hirt, U. H.; Schuster, M. F. H.; French, A. N.; Wiest, O. G.; Wirth, T. *Eur. J. Org. Chem.* **2001**, 1569–1579. (f) Ochiai, M.; Takaoka, Y.; Masaki, Y. *J. Am. Chem. Soc.* **1999**, *121*, 9233–9234. (g) Ladziata, U.; Carlson, J.; Zhdankin, V. V. *Tetrahedron Lett.* **2006**, *47*, 6301–6304. (h) Fujita, M.; Okuno, S.; Lee, H. J.; Sugimura, T.;

- Okuyama, T. *Tetrahedron Lett.* **2007**, *48*, 8691–8694. (i) Boppiseti, J. K.; Birman, V. B. *Org. Lett.* **2009**, *11*, 1221–1223.
5. (a) Dohi, T.; Maruyama, A.; Takenaga, N.; Senami, K.; Minamitsuji, Y.; Fujioka, H.; Caemmerer, S. B.; Kita, Y. *Angew. Chem. Int. Ed.* **2008**, *47*, 3787–3790. (b) Dohi, T.; Takenaga, N.; Nakae, T.; Toyoda, Y.; Yamasaki, M.; Shiro, M.; Fujioka, H.; Maruyama, A.; Kita, Y. *J. Am. Chem. Soc.* **2013**, *135*, 4558–4566.
6. (a) Altermann, S. M.; Richardson, R. D.; Page, T. K.; Schmidt, R. K.; Holland, E.; Mohammed, U.; Paradine, S. M.; French, A. N.; Richter, C.; Bahar, A. M.; Witulski, B.; Wirth, T. *Eur. J. Org. Chem.* **2008**, 5315–5328. (b) Quideau, S.; Lyvinec, G.; Marguerit, M.; Bathany, K.; Ozanne-Beaudenon, A.; Buffeteau, T.; Cavagnat, D.; Chenede, A. *Angew. Chem. Int. Ed.* **2009**, *48*, 4605–4609. Recent examples for hypervalent iodine catalysis: (c) Fujita, M.; Yoshida, Y.; Miyata, K.; Wakisaka, A.; Sugimura, T. *Angew. Chem. Int. Ed.* **2010**, *49*, 7068–7071. (d) Röben, C.; Souto, J. A.; Gonzáles, Y.; Lishchynskiy, A.; Muñiz, K. *Angew. Chem. Int. Ed.* **2011**, *50*, 9478–9482. (e) Fujita, M.; Mori, K.; Shimogaki, M.; Sugimura, T. *Org. Lett.* **2012**, *14*, 1294–1297. (f) Kong, W.; Feige, P.; Haro, T. de; Nevado, C. *Angew. Chem. Int. Ed.* **2013**, *52*, 2469–2473. (g) Shimogaki, M.; Fujita, M.; Sugimura, T. *Eur. J. Org. Chem.* **2013**, 7128–7138. (h) Bosset, C.; Coffinier, R.; Peixoto, P. A.; El Assal, M.; Miqueu, K.; Sotiropoulos, J.-M.; Pouységu, L.; Quideau, S. *Angew. Chem. Int. Ed.* **2014**, *53*, 9860–9864. (i) Basdevant, B.; Legault, C. L. *Org. Lett.* **2015**, *17*, 4918–4921. (j) Murray, S. J.; Ibrahim, H. *Chem. Commun.* **2015**, *51*, 2376–2379. (k) Bekkaye M.; Masson, G. *Synthesis* **2016**, *48*, 302–312. (l) Ahmad, A.; Silva, L. F. *J. Org. Chem.* **2016**, *81*, 2174–2181. (m) Feng, Y.; Huang, R.; Hu, L.; Xiong, Y.; Coeffard, V. *Synthesis* **2016**, 2637–2644. (n) Banik, S. M.; Medley, J. W.; Jacobsen, E. N. *Science* **2016**, *353*, 51–54. (o) Woerly, E. M.; Banik, S. M.; Jacobsen, S. M. *J. Am. Chem. Soc.* **2016**, *138*, 13858–13861. (p) Shimogaki, M.; Fujita, M.; Sugimura, T. *Angew. Chem. Int. Ed.* **2016**, *55*, 15797–15801. (q) Muñiz, K.; Barreiro, L.; Romero, R. M.; Martínez, C. *J. Am. Chem. Soc.* **2017**, *139*, 4354–4357. (r) Hempel, C.; Maichle-Mössmer, C.; Peric, M. A.; Nachtsheim, B. *J. Adv. Synth. Catal.* **2017**, *359*, 2931–2941. (s) Ogasawara, M.; Sasa, H.; Hu, H.; Amano, Y.; Nakajima, H.; Takenaga, N.; Nakajima, K.; Kita, Y.; Takahashi, T.; Dohi, T. *Org. Lett.* **2017**, *19*, 4102–4105. (t) Hashimoto, H.; Shimazaki, Y.; Omatsu, Y.; Maruoka, K. *Angew. Chem. Int. Ed.* **2018**, *57*, 7200–7204. (u) Ding, Q.; He, H.; Cai, Q. *Org. Lett.* **2018**, *20*, 4554–4557. (v) Antien, K.; Pouységu, L.; Deffieux, D.; Massip, S.; Peixoto, P.; Quideau, S. *Chem. Eur. J.* **2019**, *25*, 2852–2858.

7. (a) Uyanik, M.; Yasui, T.; Ishihara, K. *Angew. Chem. Int. Ed.* **2010**, *49*, 2175–2177. (b) Uyanik, M.; Yasui, T.; Ishihara, K. *Tetrahedron* **2010**, *66*, 5841–5851.
8. (a) Uyanik, M.; Yasui, T.; Ishihara, K. *Angew. Chem. Int. Ed.* **2013**, *52*, 9215–9218. (b) Uyanik, M.; Yasui, T.; Ishihara, K. *J. Org. Chem.* **2017**, *82*, 11946–11953. (c) Uyanik, M.; Sasakura, N.; Mizuno, M.; Ishihara, K. *ACS Catal.* **2017**, *7*, 872–876. (d) Suzuki, T.; Watanabe, S.; Uyanik, M.; Ishihara, K.; Kobayashi, S.; Tanino, K. *Org. Lett.* **2018**, *20*, 3919–3922.
9. (a) Farid, U.; Wirth, T. *Angew. Chem. Int. Ed.* **2012**, *51*, 3462–3465. (b) Mizar, P.; Niebuhr, R.; Hutchings, M.; Farooq, U.; Wirth, T. *Chem. Eur. J.* **2016**, *22*, 1614–1617. (c) Farid, U.; Malmedy, F.; Claveau, R.; Albers, L.; Wirth, T. *Angew. Chem. Int. Ed.* **2013**, *52*, 7018–7022. (d) Brown, M.; Kumar, R.; Rehbein, J.; Wirth, T. *Chem. Eur. J.* **2016**, *22*, 4030–4035. (e) Malmedy, F.; Wirth, T. *Chem. Eur. J.* **2016**, *22*, 16072–16077. (f) Mizar, P.; Wirth, T. *Angew. Chem. Int. Ed.* **2014**, *53*, 5993–5997.
10. (a) Zhang, D.-Y.; Xu, L.; Wu, H.; Gong, L.-Z. *Chem. Eur. J.* **2015**, *21*, 10314–10317. (b) Gelis, C.; Dumoulin, A.; Bekkaye, M.; Neuville, L.; Masson, G. *Org. Lett.* **2017**, *19*, 278–281. (c) Haubenreisser, S.; Wöste, T. H.; Martínez, C.; Ishihara, K.; Muñiz, K. *Angew. Chem. Int. Ed.* **2016**, *55*, 413–417. (d) Muñiz, K.; Fra, L. *Synthesis* **2017**, 2901–2096.
11. (a) Monár, I. G.; Gilmour, R. J. *Am. Chem. Soc.* **2016**, *138*, 5004–5007. (b) Jain, N.; Xu, S.; Ciufolini, M. A. *Chem. Eur. J.* **2017**, *23*, 4542–4546. (c) Jain, N.; Ciufolini, M. A. *Synthesis* **2018**, *51*, 3322.

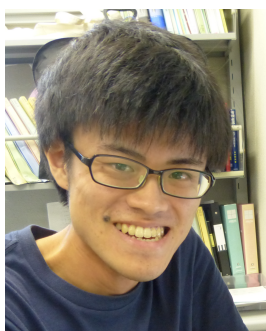
### Appendix

#### Chemical Abstracts Nomenclature (Registry Number)

- (*R*)-1-Amino-2-propanol: 2-Propanol, 1-amino-, (*2R*)-; (2799-16-8)  
 Triethyl amine, Et<sub>3</sub>N: Ethanamine, *N,N*-diethyl-; (121-44-8)  
 Di-*tert*-butyl decarbonate, Boc<sub>2</sub>O: Dicarboxylic acid, bis(1,1-dimethylethyl) ester; (24424-99-5)  
 2-Iodoresorcinol: 1,3-Benzenediol,2-iodo-; (41046-67-7)  
 Triphenylphosphine, Ph<sub>3</sub>P: Phosphine, triphenyl-; (603-35-0)  
 Diisopropyl azodicarboxylate, DIAD: 1,2-Diazenedicarboxylic acid, 1,2-bis(1-methylethyl) ester; (2446-83-5)  
 Trifluoroacetic acid: Acetic acid, trifluoro-; (76-05-1)  
 4-Dimethyl aminopyridine, DMAP; (1122-58-3)  
 2,4,6-Trimethylbenzoyl chloride, MesCOCl; (938-18-1)



Prof. Muhammet Uyanik was born in Samsun, Turkey, in 1981 and received his Ph.D. from Nagoya University, Japan, in 2007 under the direction of Professor Kazuaki Ishihara. He was appointed as an Assistant Professor at Nagoya University in 2007, and he became Associate Professor in 2020. His research focused on the development of halogen-based catalysis for the oxidative transformations.



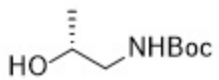
Shinichi Ishizaki was born in Mie, Japan, in 1996. He received his Bachelor's degree from Nagoya University in 2018. He is continuing his graduate studies at Nagoya University under the supervision of Professors Kazuaki Ishihara and Muhammet Uyanik. His research focused on the chiral organoiodine catalysis.



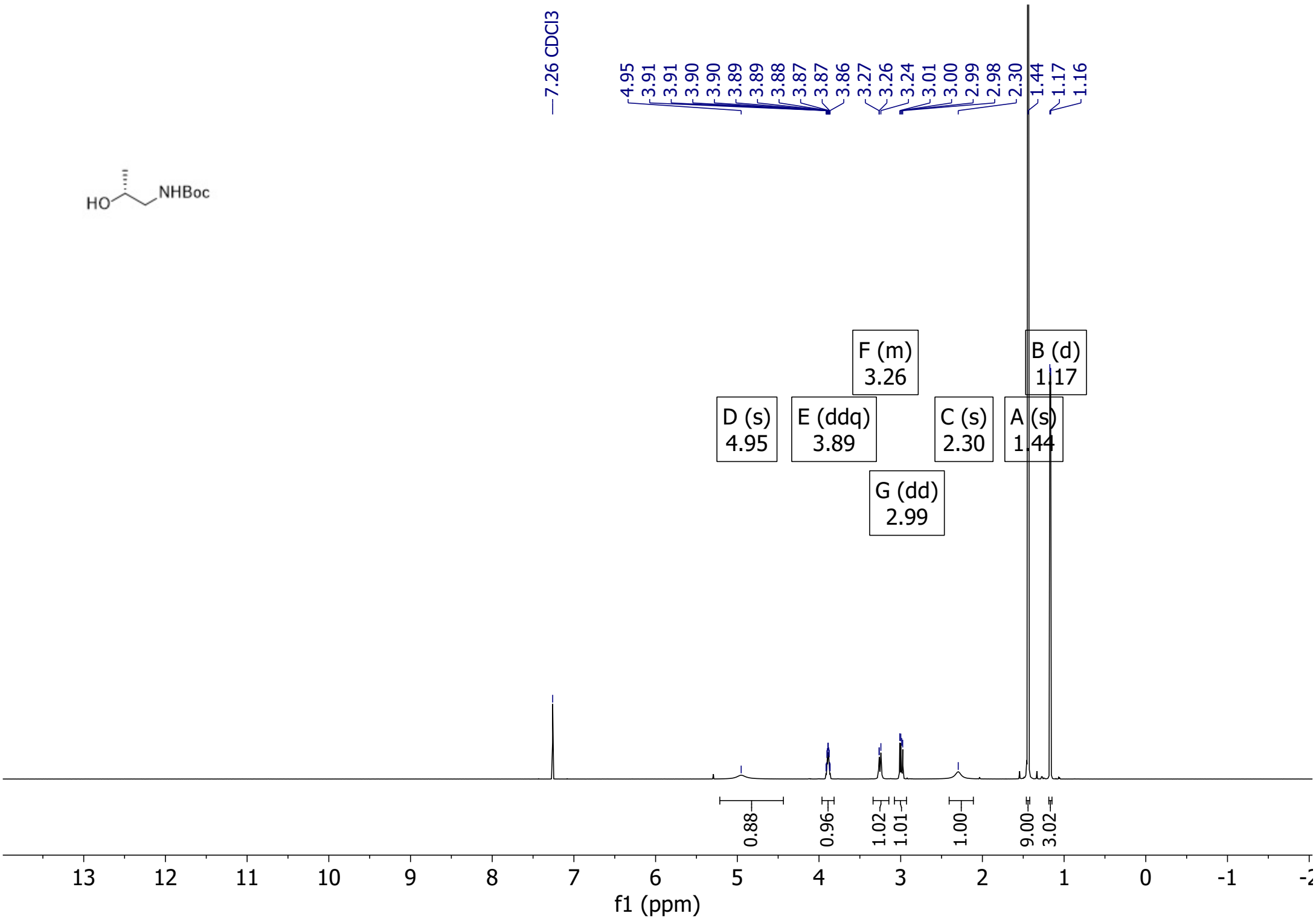
Prof. Kazuaki Ishihara received his Ph.D. from Nagoya University in 1991 under the direction of Professor Hisashi Yamamoto. He had the opportunity to work under the direction of Professor Clayton H. Heathcock at the University of California, Berkeley, for three months in 1988. After completing his postdoctoral studies with Professor E. J. Corey at Harvard University, he joined Professor H. Yamamoto's group at Nagoya University as an assistant professor in 1992, and he became associate professor in 1997. In 2002, he was appointed to his current position as a full professor. His research interest is the rational design of high-performance catalysts based on acid–base combination chemistry.

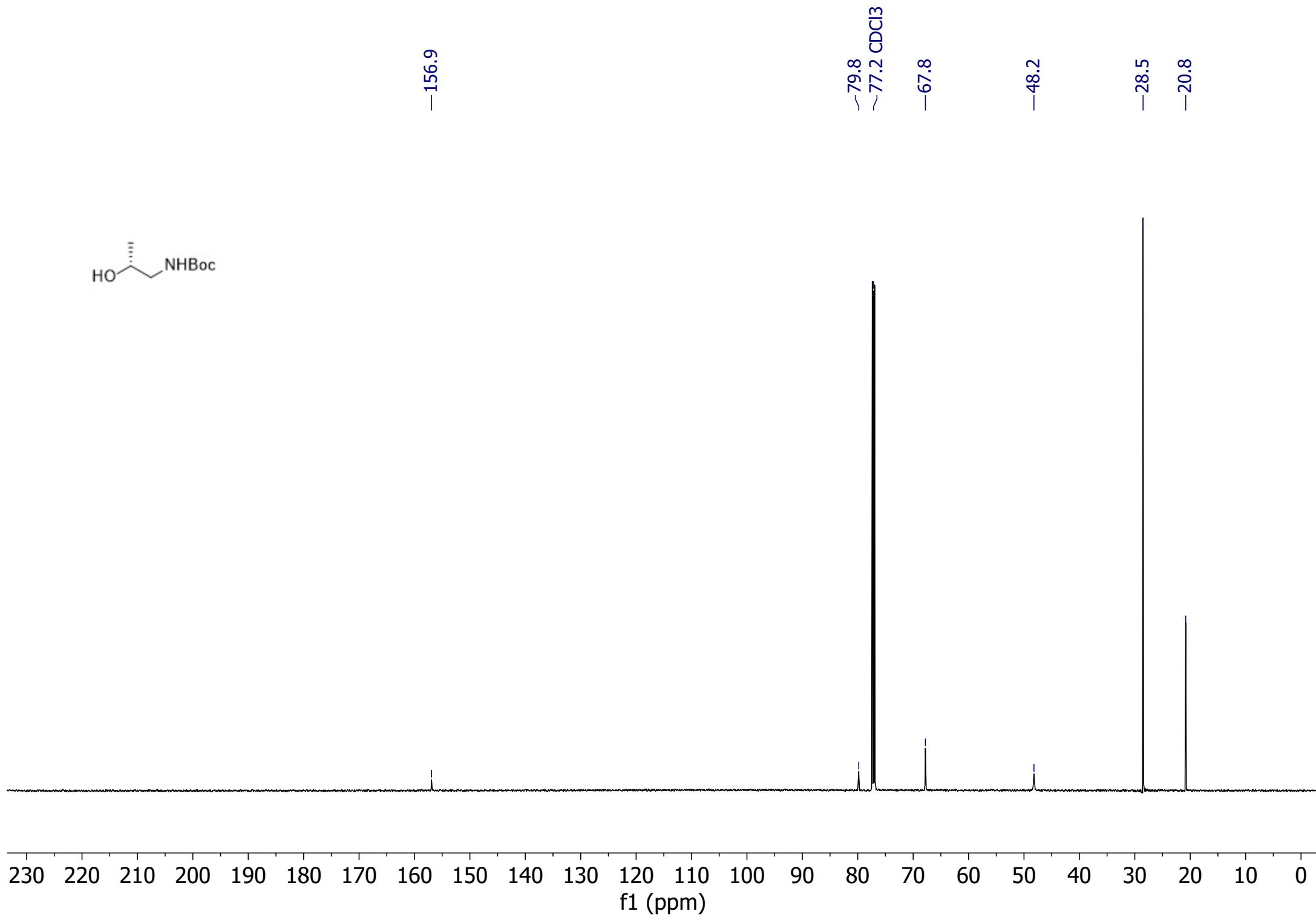
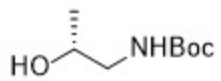


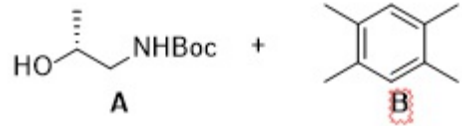
Cayetana Zarate received her B.Sc. in 2012 from the University of Valladolid (Spain). She pursued doctoral studies with Professor Ruben Martin in the area of nickel-catalyzed activation of 'inert' C–O, C–H and C–F bonds. After receiving her Ph.D. in 2017, Cayetana moved to the United States for a postdoctoral appointment with Professor Paul Chirik at Princeton University. In collaboration with Merck & Co., Inc., she designed catalysts for the isotopic radiolabeling of drug candidates. In 2019, Cayetana joined the Merck Discovery Process Chemistry Team in Boston, where her research involves the delivery of innovative chemistry that enables acceleration of drug discovery and development.



—7.26 CDCl<sub>3</sub>



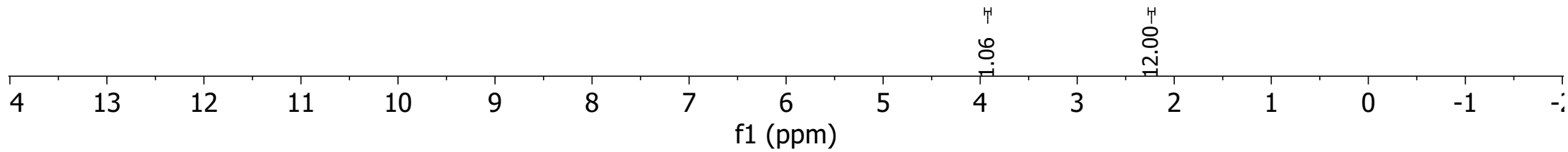
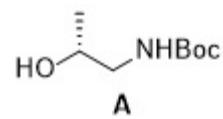
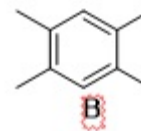


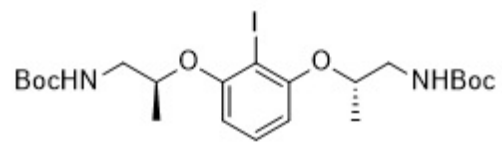


A/B ratio: 1.08 : 1.00

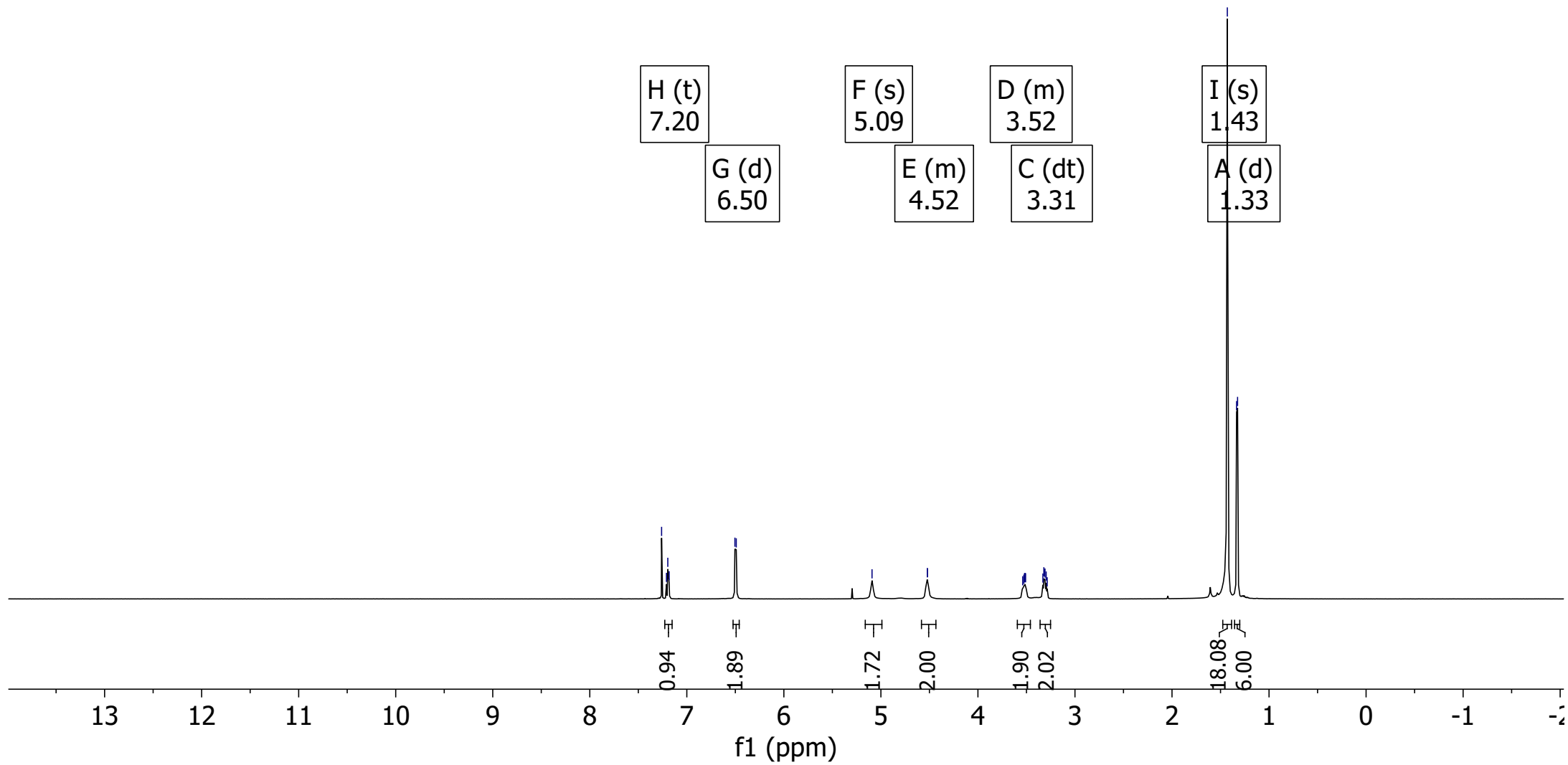
3.95  
3.94  
3.94  
3.93  
3.93  
3.92  
3.92  
3.91  
3.91  
3.90

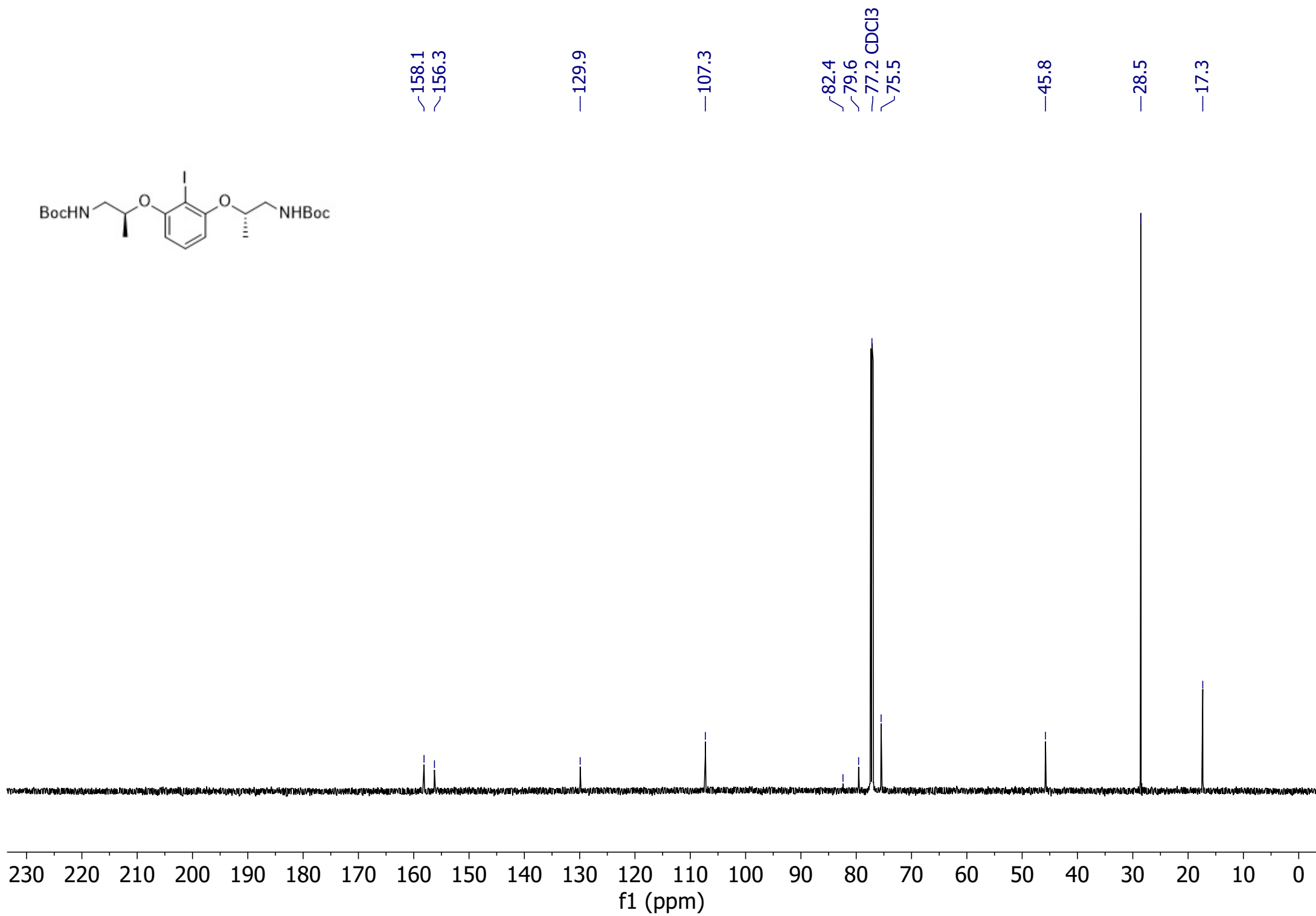
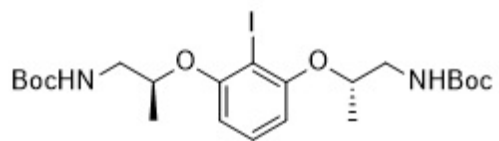
2.24

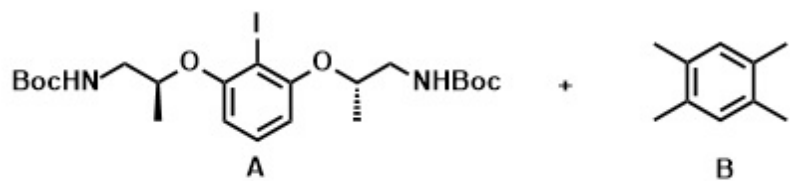




7.26 CDCl<sub>3</sub>  
 7.21  
 7.20  
 7.18  
 6.50  
 6.49  
 — 5.09  
 4.52  
 4.52  
 3.54  
 3.53  
 3.52  
 3.52  
 3.51  
 3.33  
 3.32  
 3.31  
 3.30  
 3.29  
 1.43  
 1.33  
 1.32

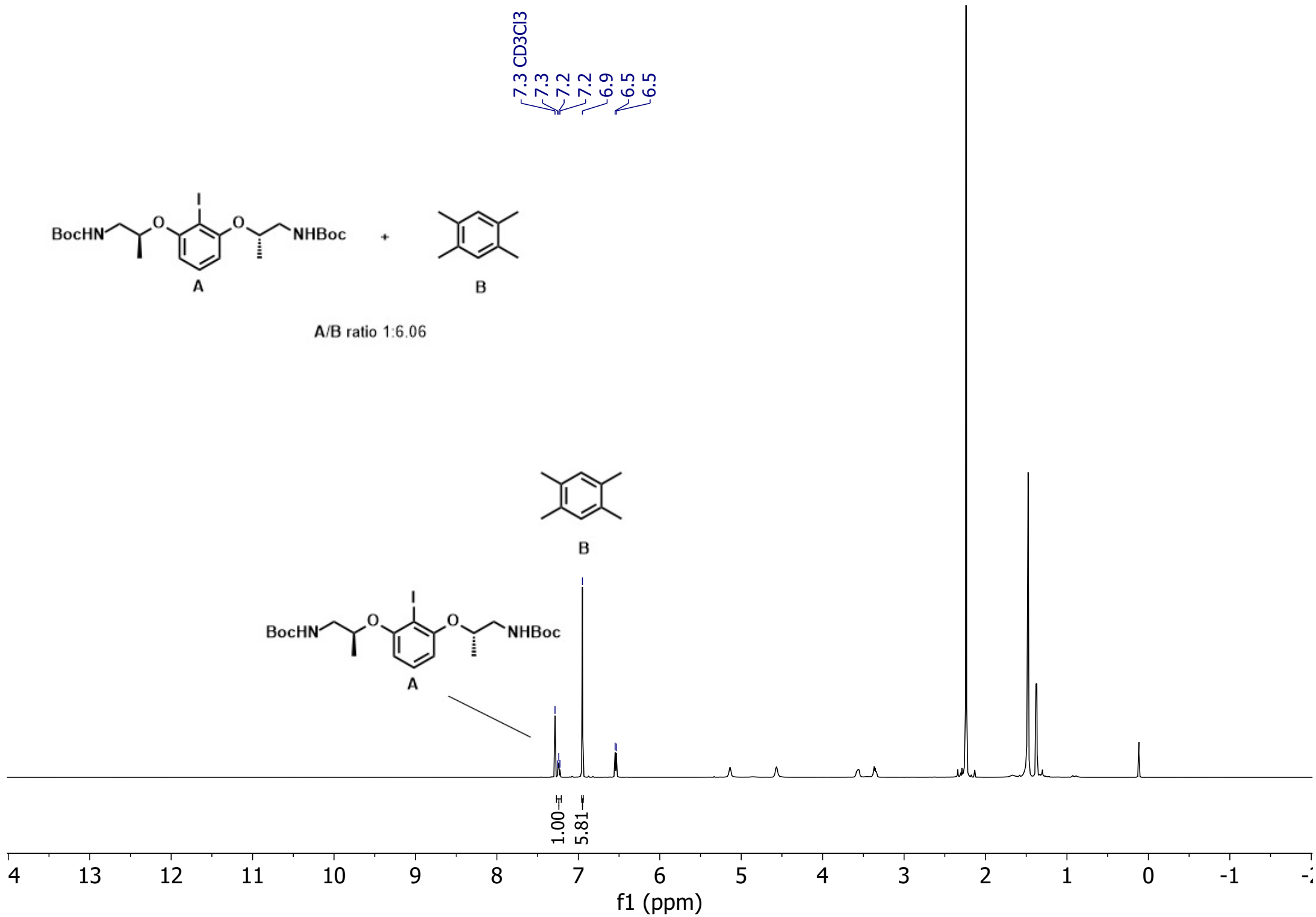


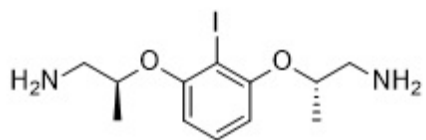




A/B ratio 1:6.06

7.3 CD3Cl3  
 7.3  
 7.2  
 7.2  
 6.9  
 6.5  
 6.5





7.26 CDCl<sub>3</sub>

7.07

7.06

7.04

6.37

6.35

4.27

4.26

4.25

4.25

4.24

4.23

3.58

2.82

2.80

2.79

2.79

2.78

2.76

2.76

1.19

1.18

A (t)  
7.06

B (d)  
6.36

C (h)  
4.25

E (s)  
3.58

D (m)  
2.79

F (d)  
1.18

1.00

2.04

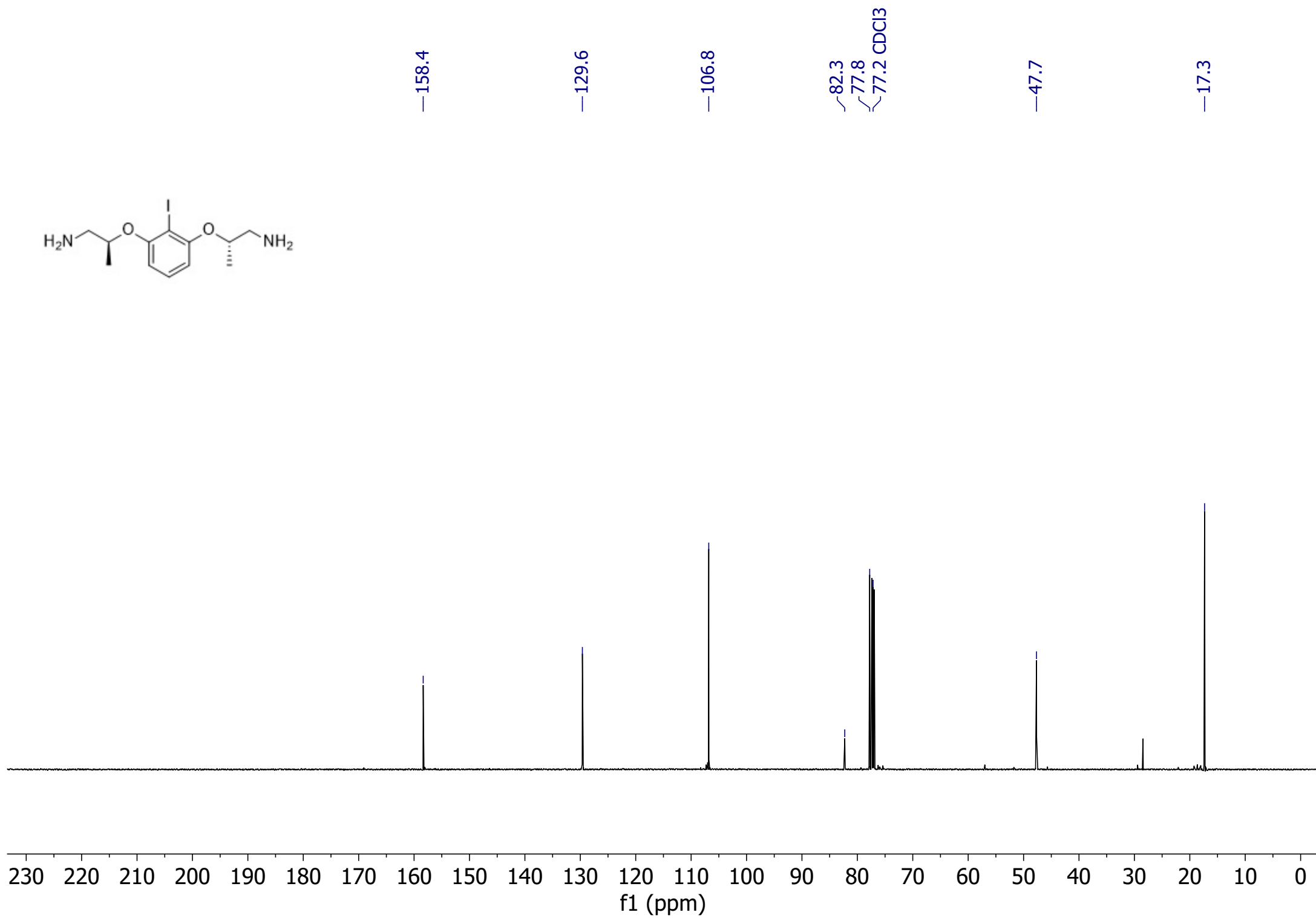
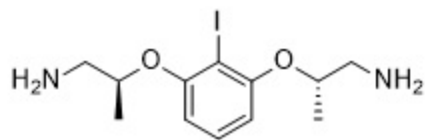
2.01

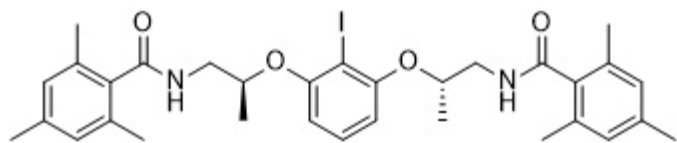
3.10

4.02

6.02

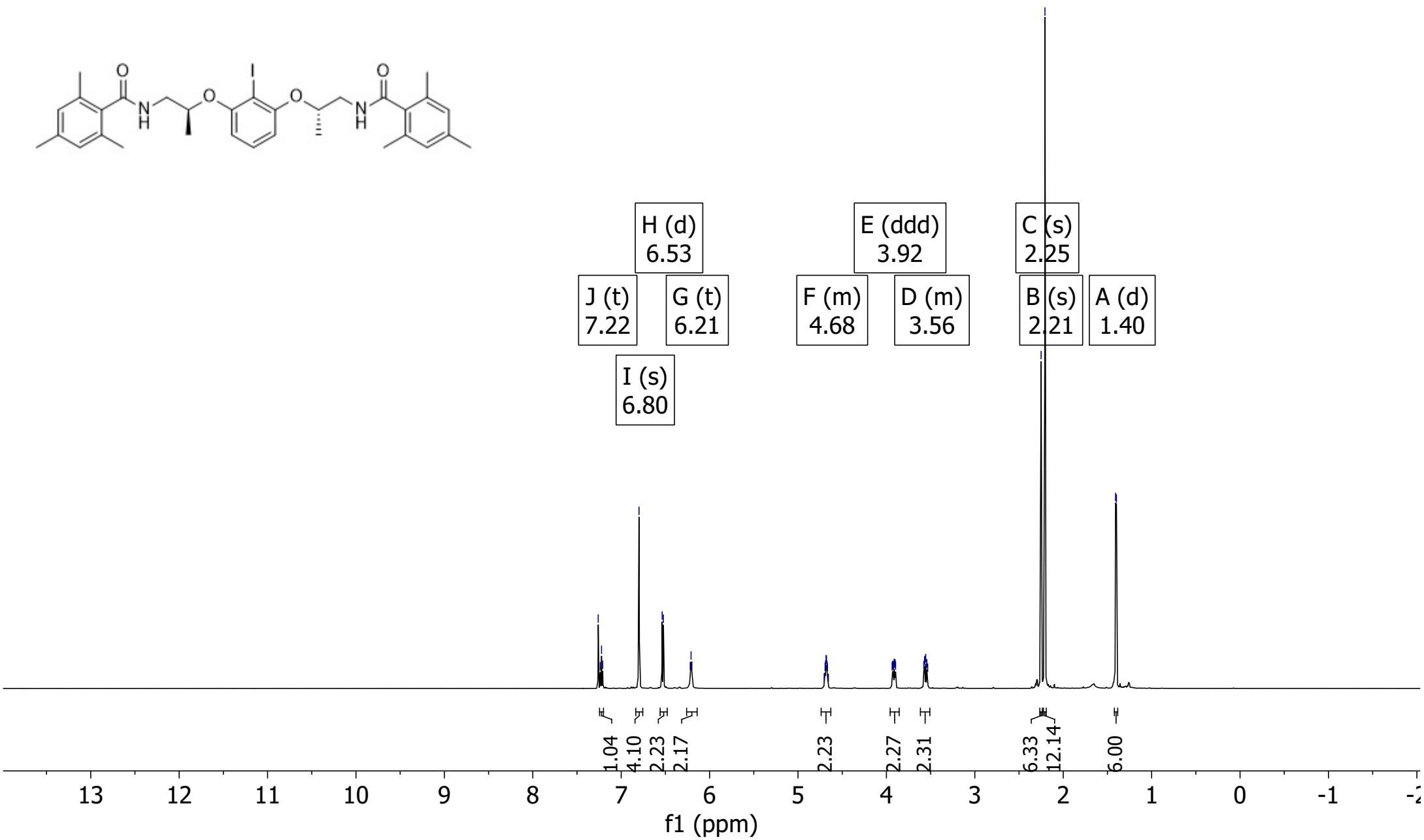
f1 (ppm)

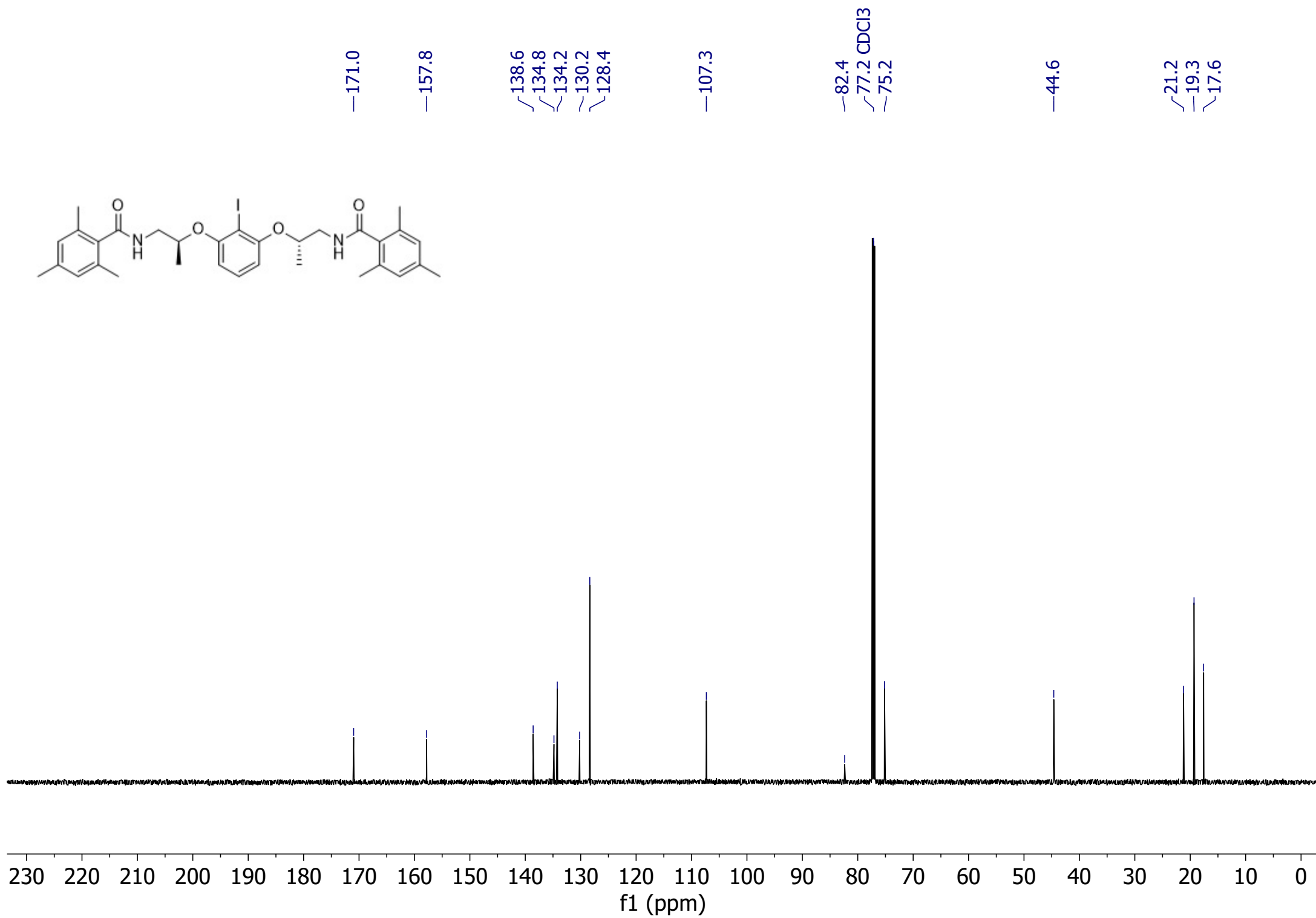
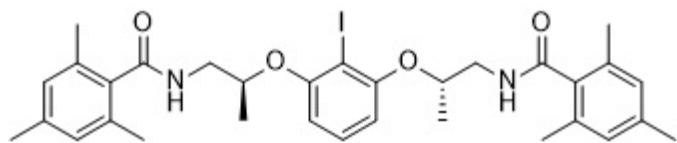


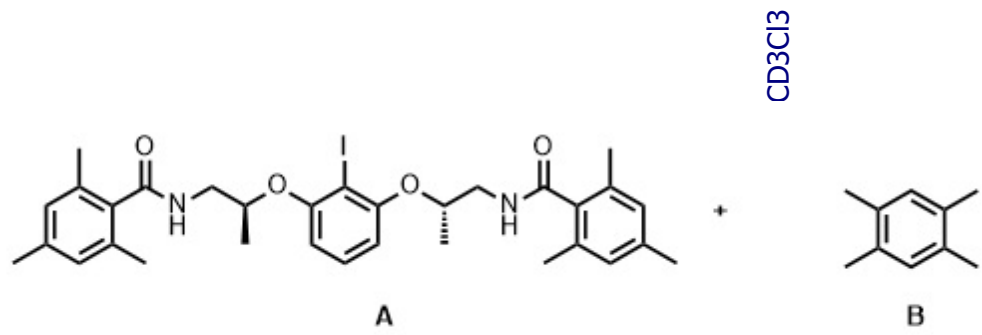


7.26 CDCl<sub>3</sub>  
 7.24  
 7.22  
 7.21  
 6.80  
 6.54  
 6.52  
 6.22  
 6.21  
 6.20  
 4.70  
 4.69  
 4.69  
 4.68  
 4.68  
 4.67  
 4.67  
 4.66  
 3.94  
 3.93  
 3.92  
 3.92  
 3.91  
 3.91  
 3.90  
 3.90  
 3.58  
 3.57  
 3.57  
 3.56  
 3.54  
 3.54  
 3.53  
 2.25  
 2.21  
 1.41  
 1.40

H (d)  
6.53  
 J (t)  
7.22  
 G (t)  
6.21  
 I (s)  
6.80  
 F (m)  
4.68  
 E (ddd)  
3.92  
 D (m)  
3.56  
 C (s)  
2.25  
 B (s)  
2.21  
 A (d)  
1.40







A/B ratio 1:4.03

